Role of Spatial Constraints on fragmentation

A dissertation submitted in the partial fulfillment of requirement for the award of the Degree of

Masters of Science
in
Physics

Submitted by
Pallavi Gupta
Roll no.-300904008

Under the esteemed guidance of
Dr. Suneel Kumar
(Assistant Professor)

School of Physics and Materials Science
Thapar University
Patiala (Punjab)-147 004

July 2011.

Dedicated to

My family

CERTIFICATE

This is to certify that the report entitled ***'Role of Spatial Constraints on fragmentation'*** submitted by ***Ms. Pallavi Gupta (Roll no. 300904008)*** of M.Sc (Physics), Thapar University, Patiala, was carried out by her under my supervision. She have not submitted this material for credit towards any other degree at Thapar University, Patiala or any other Universty.

S Kumar
15/7/11

(Dr. Suneel Kumar)

Assistant Professor,
School of Physics and Materials Science,
Thapar University
Patiala.

(Dr. O.P. Pandey)

(Prof.& Head)
School of Physics and Materials Science,
Thapar University,
Patiala.

(Dr. S.K. Mohapatra)

Dean of Academic Affairs
Thapar University,
Patiala.

Dated: 15/7/2011
Place: Thapar University, Patiala.

ACKNOWLEDGEMENT

With deep sense of gratitude, I thank all those who have contributed the conception origin and nurturing of this project.

I would like to express my sincere thanks to my project guide, ***Dr. Suneel Kumar*** Assistant Professor, School of Physics and Materials Science, Thapar Universty, Patiala for providing me valuable guidance during the entire project and for providing me his timely support, help and encouragement. His guidance & suggestions were very helpful to shape my research skill. I am sure that the knowledge gained through my association with my supervisor shall go a long way in helping me to redize goals in my life.

I am deeply indebted to ***Mrs. Varinderjit Kaur, Karan Singh Vinayak and Anupriya jain*** research scholars for providing me valuable guidance & his timely support.

I would like to express my sincere regards to ***Dr. O.P. Pandey,*** Professor and Head, School of Physics and Materials Science for providing me facilities without which this work would not be possible.

I would like to put my heartiest gratitude to my whole family for their constant support enthusiasm and encouragement.

In last but not the least I would like to thank my friends Rubina and Deepinder and all those people who have helped me directly or indirectly to do my project work.

Pallavi Gupta

Ms. Pallavi Gupta
Roll no: 300904008

Date:15/7/2011
Place: Thapar Universty, Patiala.

Abstract

In the present study, we review the formation of fragments in Au+Au, Xe+Xe, Ne+Ne reaction at two different incident energies at E=100 MeV/nucleon and 600 MeV/nucleon. For the present analysis, IQMD model has been used as an event generator. To find the best clusterization spatial constraints for the formation of fragments minimum spanning tree method has been applied at constant momentum constraint by varying the distance among the nucleons. We expect the present study will give us an optimize value to form the stable fragment.

TABLE OF CONTENTS

Page no.

Certificate……..(iii)

Acknowledgement…….(iv)

Abstract……..(v)

Contents…….(vi)

List of Figure……(viii)

Chapter-1 Introduction

1.1 Low, Intermediate and High energy Physics ….....2

1.2 What happen in heavy ion collision? …….4

1.3 Nuclear Equation of State……...5

1.4 Multifragmentation……..7

1.5 Theoretical view of Multi-fragmentation…….....8

1.6 Experimental view of Multi-fragmentation……...10

1.7 spatial correlations……..……...……12

1.8 Momentum dependent interactions……13

Chapter-2 Methodology

2.1 QMD Model……..…....15

2.2 IQMD Model…….....16

2.3 Initialization……..17

2.4 Propagation……...…..17

2.5 Potentials used in IQMD……..18

2.6 Collision……..20

2.7 Method of clusterization……..21

Chapter-3 Spatial Correlation

3.1 Introduction……..23

3.2 Phase Space Analysis……23

3.3 Time evolution of nucleon- nucleon collision……...26

3.4 Time evolution of Free nucleons……...28

3.5 Time evolution of light mass fragments……28

3.6 Variation of various fragments with space correlation ……....31

3.7 Multiplicity of IMF's with Scaled Impact Parameter ……..36

3.8 Energy dependence of the light mass fragments……...38

3.9 Energy dependence of the intermediate mass fragments ……40

3.10 Dependence of various fragments on total mass of the system ……..40

3.11 Comparison with experimental data ……...……43

Chapter-4 Summary and outlook……45

References……46

LIST OF FIGURE

Fig.1.1. phase diagram of nuclear matter shows the fundamentally different states that have been conjectured.

Fig.1.2. Initialized projectile and target nuclei at time t=0fm/c.

Fig.1.3. Two nuclei during collision.

Fig.1.4. Two nuclei after the collision.

Fig.1.5. Two nuclei collide to form compound nucleus and then fragmented.

Fig.3.1. Phase space distribution of the projectile and target nucleons without (left) and with momentum dependent interactions (right) in X-Z plane. The reaction under study is $_{79}Au^{197}$ + $_{79}Au^{197}$ at incident energy E = 100 MeV/nucleon for semi-peripheral geometry. The panels from top to bottom are representing the positions at different times.

Fig.3.2. Momentum phase space distribution of the projectile and target nucleons without (left) and with momentum dependent interactions (right) in P_X-P_Z plane. The reaction under study is $_{79}Au^{197}$ + $_{79}Au^{197}$ at incident energy E = 100 MeV/nucleon for semi-peripheral geometry. The panels from top to bottom are representing the positions at different times.

Fig.3.3. Allowed collision as a function of the time. The top and bottom panel represents the reaction at 100 MeV/nucleon. The top and bottom panel represent, respectively, the central collision ˆb = 0 and peripheral collision ˆb = 0.6. The left panel represent the reaction for without MDI and right panel represent reaction with moment dependent Interaction.

Fig.3.4. Multiplicity of free nucleon (A=1) for central collision for soft EOS.

Fig.3.5 Multiplicity of free nucleon (A=1) at central collision for SMD EOS.

Fig.3.6. Multiplicity of light mass fragments ($2<A<4$) at central collision for soft EOS.

Fig.3.7. Variation of Multiplicity of free nucleon as function of R_{clus} (fm) for central collision.

Fig.3.8. Variation of multiplicity of LMF's as function of R_{clus}(fm) for central collision.

Fig.3.9. Variation of Multiplicity of IMF's as a function of R_{clus} (fm) for central collision.
Fig.3.10.Multiplicity of IMF's of $^{197}Au_{79}+^{197}Au_{79}$ and $^{91}Zr_{40}+^{91}Zr_{40}$.
Fig.3.11.Multiplicity of light mass fragments as a function of energy at central and semi-central collision.
Fig.3.12.Multiplicity of intermediate mass fragments as a function of energy at central and semi-central collision.
Fig.3.13.Multiplicity of LMF's & IMF's as a function of total mass of the system.
Fig.3.14.Multiplicity of IMF's as function of Z_{bound}.

Chapter 1

Introduction

Nuclear physics (at low/intermediate/high energies) is one of the most extensively studied fields. The nuclei used as beam of particles are generally completely ionized. After many decades, nuclear physics has been categorized into different branches. It has been categorized in four branches which are given as:

- Deconfinement and quark gluon plasma.
- Low energy γ-ray spectroscopy.
- Nuclear collectivity through giant resonances.
- Intermediate energy heavy ion reactions.

In the last three decades lot of efforts have been made experimentally as well theoretically to understand the nuclear physics at intermediate energies ranging from 10 MeV/nucleon to 2 GeV/nucleon.

In nuclear physics, the nuclei used as beam of particles are generally completely ionized. The nuclei can be directed to a fixed target, or can be split into two beams moving in opposite directions that are brought into collision at a well-defined spot.

The heavy ion collision is a collision, when atomic nuclei, generally called heavy ion collide at very high energy such that the kinetic energy exceeds significantly the rest mass energy and many strongly interacting particle are produced. The term heavy ion is used for the nucleus more massive than helium or we can say that the nuclei having A>4. The branch of physics which deals with the phenomenon that occur when two heavy nuclei are brought into close contact such that nuclear forces that hold the neutrons and protons together within the nucleus is called heavy ion physics[1].

1.1 Low, Intermediate and High energy physics

Main interest to study the low energy nuclear physics ($\leq$ **10MeV/nucleon**) or heavy ion collisions is to look for the low density phenomena. The low energy heavy-ion reactions give unique possibility to look for the nuclear interactions, fusion-fission, cluster radioactivity, formation of super heavy nuclei, possibilities of synthesis of super heavy elements, halo nuclei [2-5] etc. Low energy nuclear physics research concerns itself with understanding the structure and stability of the nuclei in the world around us as well as the reactions which formed them in the cosmos. The reaction cross section at low energies composes of three categories i.e., the fusion, quasi-elastic and deep inelastic scattering [5]. All these processes depend on the projectile-target combinations, on the bombarding energy of projectile and angular momentum. Due to large efforts in low energies heavy ion collisions, the understanding of different phenomena is quite rich.

At low energies the available free phase space is very small, therefore 98% of attempted collisions are blocked the whole dynamics at low energies is due to the mean field. Because at low incident energies the nucleon-nucleon collisions are negligible and mean field is maximum[6].

With the passage of time, one was able to accelerate the heavy-ion with the bombarding energies comparable to its rest mass. Thus the new dimensions which are termed as intermediate and relativistic energy heavy-ion physics came to existence. The main interest to study the heavy-ion collisions is the investigation of the properties of nuclear matter at extreme densities and excitation energies. The study of the behavior of the hadrons in hot and dense nuclear matter is one of the central topics in present day research. Naturally like all other materials, the properties of nuclear matter are also influenced by the pressure, density and temperature. The hadronic matter may have rich structure in this unexplored domain of high excitation energies and compressions.

At relativistic energies ($\geq$2 GeV/nucleon) there is a presence of large free phase space, so only 4% of attempted collisions are blocked and the dynamics is termed as cascade approach. Whereas at intermediate energies, both the cascade picture as well the mean field are taken into consideration.

The study of intermediate energy heavy-ion collision needs correct treatment of the real and imaginary parts of nuclear interactions. The real part influences the trajectory of nucleons whereas the imaginary part deals with nucleon-nucleon collisions.

As indicated in the figure, there are conjunctions about a nuclear liquid-vapour phase transition at low temperature and sub-nucleonic densities. At very high densities and temperature one may have quark-gluon plasma [7], whereas at moderate temperature the hadron gas can occur. The giant resonances generate the densities which are close to the normal nuclear matter densities. The only remaining candidate is the heavy ion collisions at intermediate and relativistic energies which can compress the protons and neutrons to 2-3 times the normal nuclear matter densities and a typical temperature of 100MeV can be reached [7]. The possibility of generating the high density matter give rise to several investigation and questions. Some of these are how does nuclear matter respond when it is compressed or heated? What role do the strange particles play in hot and dense nuclear mater?

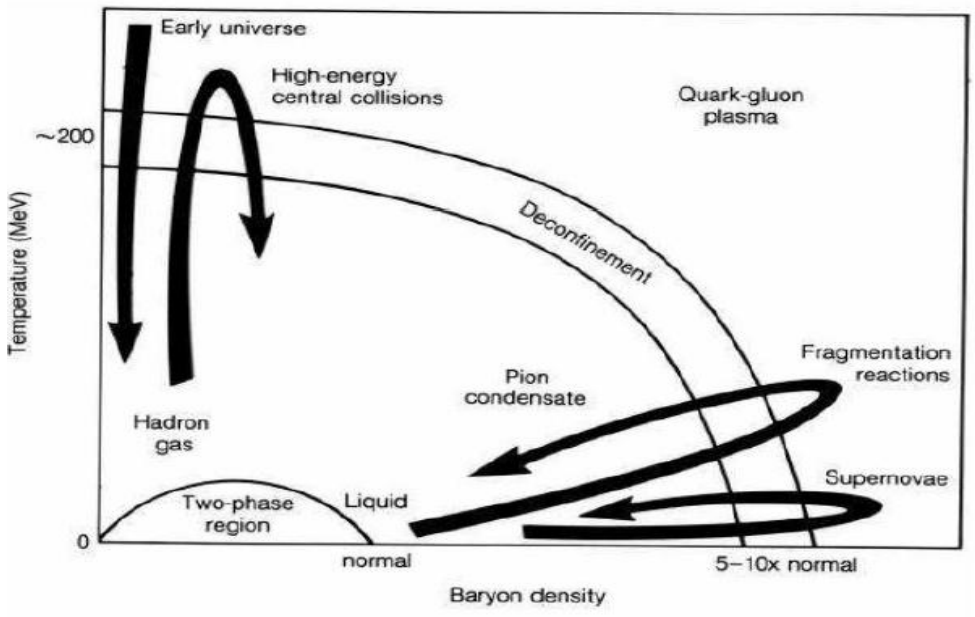

Fig.1.1. Phase diagram of nuclear matter shows the fundamentally different states that have been conjectured.

1.2 What happens in Heavy ion collision?

In above discussion, we study what is heavy ion collision and what is the main interest to study the heavy ion collision. Now our interest is to study that what happens in heavy ion collision?

In below fig.1.2, the two nuclei are approaching each other.

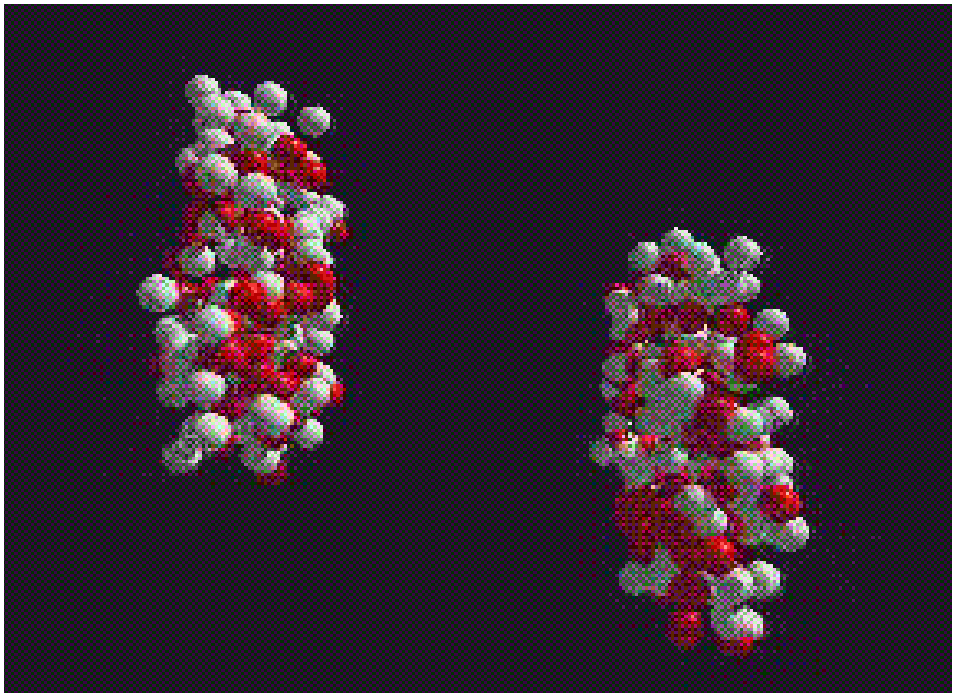

Fig.1.2. Initialized projectile and target nuclei at time t=0fm/c

If the nuclei touch, they stop each other and start to build up a hot density region. Kinetic energy is transformed into compressional energy and temperature, as shown in fig.1.3:

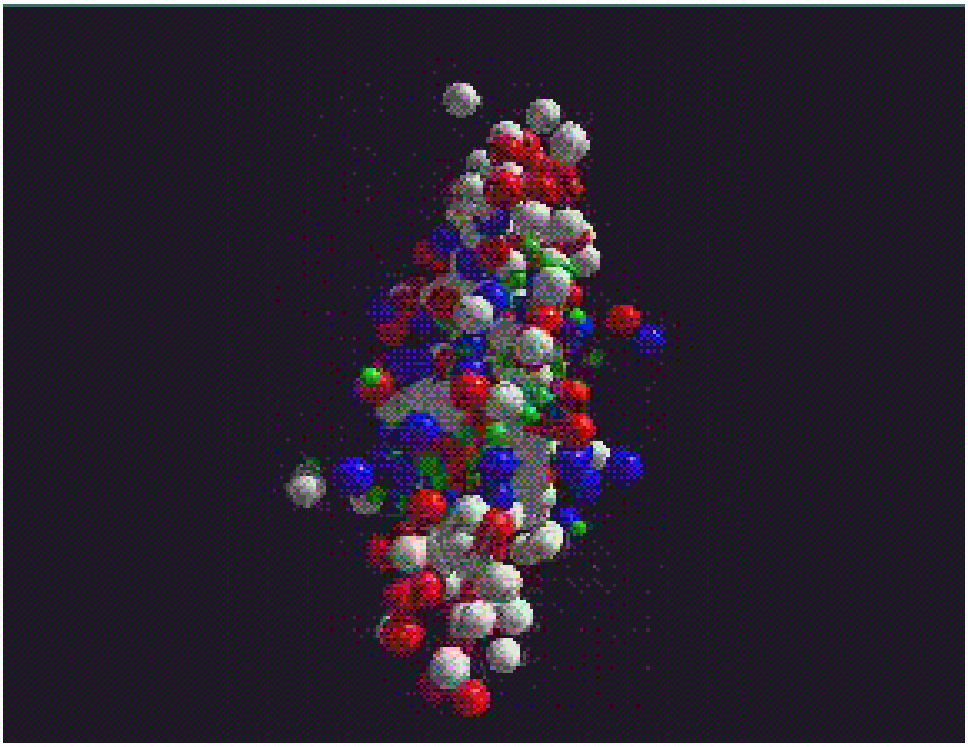

Fig.1.3. Two nuclei during collision

In this hot region a huge amount of nuclear resonances (blue) are produced. These resonances decay and produce mesons, preferentially pions. The remnants of projectile and target move off from the compressed region. The hot compressed region itself starts to expand and cool down. The nucleons, resonances & produced mesons perform further interactions (re-scattering) which may again produce other forms of resonances and mesons as shown in fig.1.4:

1.3 Nuclear Equation of State (NEOS)

The theoretical study of the NEOS deals with most of the fundamental problems of nuclear physics. Nuclear equation of state tells us about the compressibility of nuclear matter. Nuclear matter has its energetic minimum at about 0.15 to 0.17 particle per Fermi cube. If we try to change density (e.g. by compression), we have to overrule the repelling

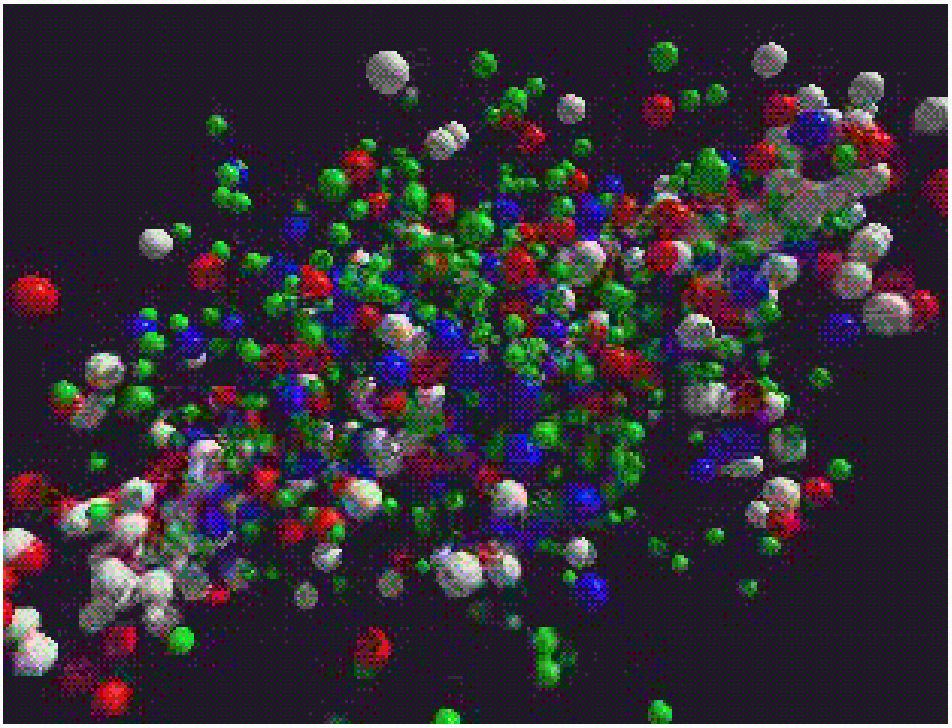

Fig.1.4. Two nuclei after the collision

The system expands more and more, and the unstable resonances decay.

forces i.e we have to pump the compreesional energy into the system. NEOS describe which compressional energy corresponds to which density. Energy per nucleon is commonly quantified in terms of nuclear incompressibility given by the equation:

$$\kappa = 9\rho_o^2 \frac{d^2}{d\rho^2}\left(\frac{E}{A}\right).$$

The value of incompressibility for soft equation of state is nearly equal to 200 MeV. If the actual value turns out to be below this value, we may consider equation of state to be soft, and stiff for opposite case.

1.4 Multifragmentation

At intermediate energy, sometime nuclear matter break into one or two fragments this process is called fission while sometimes it breaks into many fragments, this process is called multifragmentation. In words we can say that when two nuclei collide with each other they break into small and medium fragments. The produced particles in this process include the free particle, light charged particles as well as very heavy clusters. The process of multifragmentation when two nuclei collide with each other shown in fig.1.5:

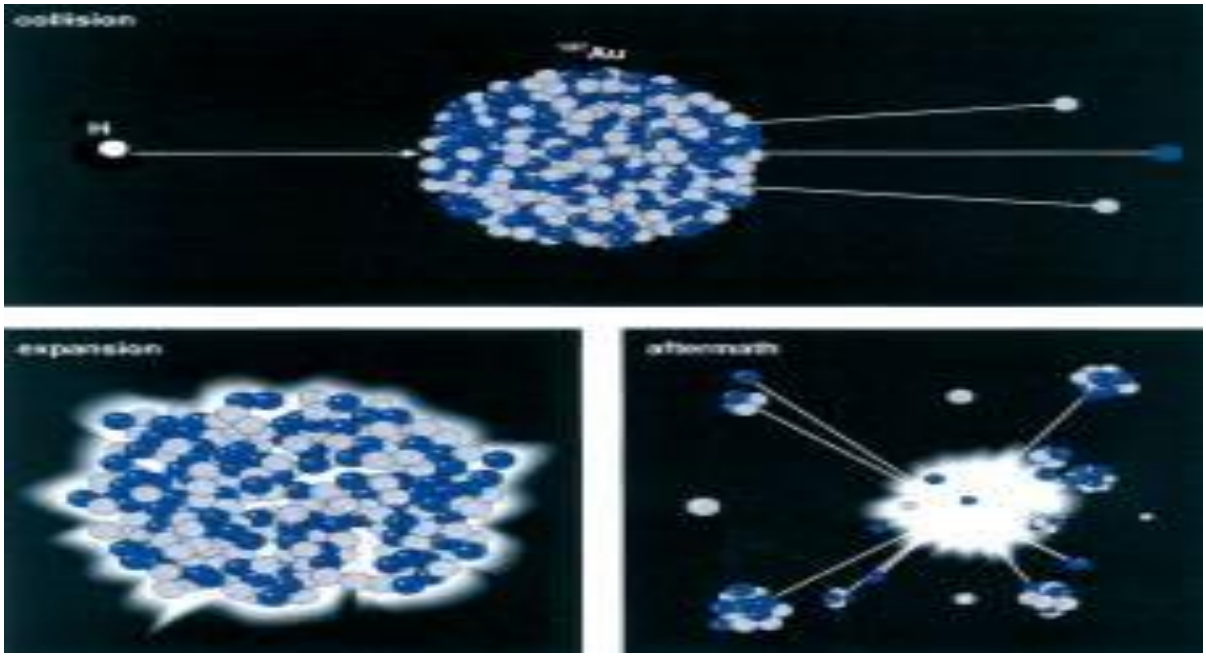

Fig.1.5. Two nuclei collide to form compound nucleus and then fragmented.

This diagram shows that at intermediate and relativistic energy, the two nuclei collide and form the compound nucleus which further decomposes into small and medium fragments. The compound nucleus formed at intermediate and relativistic energies gives information to study the nuclear matter under extreme conditions. This production of particles is linked with the incident energy and collision geometry.

Huge experimental data of multifragmentation give unique opportunity to search for the fundamental questions like origin of fragments and mechanism behind multifragmentation and the role of dynamical correlations in their formation.

1.5 Theoretical review of multifragmentation

The study of intermediate heavy-ion collision needs correct treatment of nuclear interaction. Naturally if projectile and target are comparatily same (symmetric) then reaction leads to high compression of the system whereas, asymmetric reactions lead to the heat or thermal energies. In theoretical treatment there are many objective and parameters before and after the collision in time scale on which theory can be proposed like incident energies, type of target and projectile, density and impact parameter etc before the collision and flow, rapidity, balance energy and many fluctuation and correlations etc. after the collision. In literature every model is capable of explaining the reaction dynamics to some extent.

The theoretical models for the processes at intermediate energies can be divided into two categories: Statistical and Dynamical models. Example of statistical models include multi-particle phase space models, such as the Statistical Multifragmentation Model (SMM) [8] and the Berlin Multifragmentation Model (BMM) [9], which can incorporate specific nuclear properties directly. But this model was failed in the study because of its limitations which are as:

The situation at the start of reaction is based on some assumption for the degree of thermalization. The statistical models give a better description only of the later/final stage of the reaction.

Hence due to these limitations statistical models were neglected. Therefore this study is possible by the dynamic model only.

The dynamical approaches such as the Time Dependent Hartree-Fock (TDHF) [7] or its semi-classical version called Vlasov equation (in phase space) [10] are suitable at low incident energies, where nucleon-nucleon collisions are negligible. However, a suitable and reasonable approach for the intermediate energy heavy-ion physics should treat the nucleon-

nucleon scattering and mean field on equal footing. Some attempts were made in the literature to extend the TDHF theory to take care of the residual n-n interactions, which are responsible for the two-body collisions. This was dubbed as Extended Time dependent Hartree-Fock (ETDHF) theory [11]. However, its numerical implementation prohibited its use for large scale investigations of heavy-ion collisions.

In the first attempt, semi-classical version of ETDHF theory i.e. Vlasov equation [10] was coupled with nucleon-nucleon collisions and thus, a new realization, named as Boltzmann-Uehling - Uhlenbeck equation (BUU) [12], was developed to study the large deviation problems of low, intermediate and relativistic heavy-ion collisions. The BUU equation was solved by test particle method. The one body distribution function is described as a collection of NA test particles, where A is the mass number and N is event number. All possible collisions between the test particles are considered, i.e, there is no division of test particles. In other words, N parallel runs communicate with each other, therefore, event by event correlation cannot be analyzed.

Keeping in mind the requirement of intermediate energy region, one would like to have those methods where correlations and fluctuations among nucleon can be preserved. The Classical Molecular Dynamics (CMD) [13] approach (or the equation of motion), in principle, is capable of predicting the both compression fragments production. It also incorporates the complete classical N-body dynamics which is necessary to describe the formation of the fragments. The simple Classical Molecular Dynamics models, however, needs major refinements (including quantum features). The quantum features play a very important role at low incident energies. The above approach was later extended to incorporate the quantum features by Aichelin and Stocker [7]. This new approach, which explicitly incorporates the N-body correlations as well as nuclear matter equation of state and important quantum features (like the Pauli principle, Stochastic scattering and particle production), was dubbed as Quantum Molecular Dynamics (QMD) model [14, 15].

As discussed above, the dynamical evolution of the nucleus-nucleus collisions is simulated by quantum molecular dynamics (QMD) and the Boltzmann-Uehling-Uhlenbeck (BUU) models as well as their relativistic extensions. With the development of radioactive ion-beam physics, several rather comprehensive isospin-dependent, but mostly semi-classical transport

models such as IBUU [16], SMF [17] and IQMD [1] have been successfully developed in recent years to describe nuclear reactions induced by neutron-rich nuclei at intermediate energies.

In nuclear physics, the key problem in CMD methods lies in the treatment of the Pauli principle. Nucleons are fermions and it is difficult to speak of nuclei without the Pauli principle. This question is simply overlooked in strictly classical calculations. MD methods with Pauli principle address this question but with disputable success.

Isospin dependent Quantum Molecular Dynamics: IQMD model in heavy ion collisions is used for studying the isospin effects on nuclear transverse collective flow, on nuclear radial flow and nuclear fragmentation. The dynamics in the formation of the transient state is mainly governed by three components, namely, the mean field, two body collisions, and Pauli blocking. For an isospin dependent reaction dynamics algorithm, it is essential that all the three components should reasonably include isospin degrees of freedom. In addition, it is also important that, the initialization of projectile and target nuclei, the samples of neutrons and protons in phase space should be treated separately since there exist a large difference between neutron and proton density distributions for nuclei. IQMD model is developed just on above basis. It has been shown that the IQMD can be used with large success for studying the effects of isospin in heavy ion collisions at intermediate energies.

1.6 Experimental review of multifragmentation

Earlier, one could accelerate the light ions only; therefore, the field was dominated by shooting light particles on heavy targets. As the quest grew, new and larger accelerators were built which could accelerate heavy nuclei up to several hundreds of GeV that led to the new unexplored world of nuclear physics.

Nuclear fragmentation was discovered nearly seventy three years ago[18] in cosmic ray studies as a puzzling phenomena accompanying the collision of relativistic protons with a heavy target and consisted of the emission of slow nuclear fragments. These fragments were in the range of $3 \leq Z \leq 30$, dubbed as intermediate mass fragments. Using the radiochemical

methods, total cross-section of the fragmentation could not be determined and process was considered as very rare and exotic. In 1980's, Jacobsson et. al. [19], observed the multiple emission of IMF's in the emulsion irradiated by the carbon beam at 250 MeV/nucleon. This result created the interest of the nuclear community toward multifragmentation. Warwick et.al.[20] found that multifragmentation is a dominant reaction channel at beam energies higher than 35 MeV/nucleon. Further, the Purdue group [21] conjectured that multifragmentation is a clear signature for the phase transition between a gaseous and liquid phase of nuclear matter, which occurs around a density of 0.4 ρ_0; ρ_0 is the normal nuclear matter density. Since then, the study of multifragmentation has been considered of great interest.

Experiments performed at LBL (Lawrence Berkeley Laboratory) in the early 80's yield first 4π information of the final momentum distributions in heavy-ion reactions. The first experiments at Berkley served mainly to get the experimentalists and theoreticians aware of the problems from medium energy heavy-ion collisions to nuclear equation of state. Lots of detectors included the forward and 4π designed to understand the each and every aspect in detail.

Later on, several accelerators were built at Michigan State University (USA), GANIL (France), and at GSI (Germany). The SIS (heavy ion synchrotron) accelerator at GSI is specially designed to study the heavy-ion collisions at intermediate energies. The MSU group at Michigan state university is very active in studying the fragment's spectra at lower side of the bombarding energies. Similarly efforts are also made by INDRA group at GANIL; ALADIN group at GSI has provided complete spectra of the fragments. These experiments enable precise measurements on the emission of primary and secondary particles and therefore provide a stimulating challenge to the theoretical description of heavy ion collisions.

In actual heavy-ion experiment, the crucial part of the analysis is sorting of "well measured" events as a function of the violence of the collision (i.e. impact parameter). This analysis is meant for comparing the results with experimental findings of various collaborations.

The FOPI and ALADIN group at GSI are studying the variety of reactions giving nearly all kinds of possibilities. It ranges from ^{12}C to ^{208}Pb and with incident energy between 100 MeV/nucleon and 1000 MeV/nucleon. The multiplicity of charged particles denoted by PM has often been used by the FOPI group at GSI to characterize the events. This group also used a new quantity called ERAT for sorting which is discussed in [22].

The main interest of INDRA collaboration at GANIL is to study the collisions where large multiplicities of the nucleons are observed in the exit channel and they have studied the influence of different parameters on multifragmentation including role of size of system in entrance channel, Coulomb instabilities etc.

In particular, the size effects are studied in symmetric collisions of ^{36}Ar+KCl [23], ^{58}Ni+^{58}Ni, ^{129}Xe+^{118}Sn [24], ^{181}Ta+^{197}Au and $^{92}U_{238}$+$^{92}U_{238}$

On the other hand the entrance channel effects are studied by keeping the total mass equal to 250 units. Naturally, for studying the gentle compression and Coulomb instabilities, they have to go to heavy fragments. A detailed theoretical study of INDRA experimental findings was carried out by Aichelin and coworkers [15].

1.7 Spatial correlations

In the dynamical models (QMD)[15], (MD)[25], (BUU)[12], (RQMD)[23] one start with the two well defined nuclei and then follow the time evolution of the reaction. In other worlds the correlations and fluctuations among the particles are preserved. All the dynamical models follow the dynamics of single nucleon only and no model deals with the fragments directly. One mostly chooses the time of the construction of fragments t = 200fm/c i.e. the saturation time of the reaction [15,26,27]. The method of fragment construction can vary from simple correlation to very complicated algorithm, which depends on minimization of energy [26]. Space correlation method is very fast method but it can't address the problem of time scale of fragmentation. It leads to single cluster at the time of high density. Apart from these facts it has a couple of limitation.

1. In central reactions due to nucleon-nucleon collision the initial nucleon-nucleon correlation is distorted. As a result the nucleons with large relative momentum can be close in spatial space and hence can be a part of same fragment. These fragments will be unstable and will decay in the due course of time by emitting either nucleons or light mass fragments (LMF's).
2. In peripheral collision, we have multifragmentation of spectator matter. The spectator nuclei receive energy and get excited. The excited nuclei emit light mass fragments or intermediate mass fragments. Thus much of the initial correlation is preserved and the fragments are reasonably bound. Experimentally one fails to explain fragment multiplicity at peripheral collisions. The possible reason was supposed to be that less energy may be transferred from participant zone to the spectator zone and hence spectator nucleus does not break into fragments.

However the other method depends upon the minimization of energy. The method deals with the most bound fragment configuration and hence was able to explain experimental data at peripheral collisions very nicely.

In space correlation method, at the later stage of reaction, the correlations in momentum space also play any role, if the cut in the relative momentum is $\geq$ 268 MeV/c, however this value is too large to keep the nucleons bound in a fragment. If we take the cut (nearly 150MeV/c) about the average Fermi momentum, one finds a strong effects of the cuts on fragment multiplicity and rapidity distribution in central collision where as the effect is the least for peripheral collisions.

1.8 Momentum dependent Interaction

The momentum dependence of nuclear equation of state has also attracted a lot of consideration, momentum dependent interactions are found to affect the collective flow quite drastically[28].

During the initial phase of collision, the effect of momentum dependent interaction is very strong. The particles propagating with momentum dependent interaction are accelerated in the transverse direction during the early phase of the reaction. As a result fewer collisions takes place and the transverse flow increase

considerably. To study the role of equation of state (EOS) and momentum dependent interaction (MDI) in multifragmentation, one start with simple form of nuclear EOS which has couple of parameters that are specified by global properties of nuclear matter. (i.e. by fitting the binding energy, saturation densities, etc.). The different compressibilities lead to different EOS. By simulating the heavy ion collisions with different EOS's one can study the effect of different EOS and of the momentum dependent interactions. We fix the nucleon-nucleon cross section and simulate the heavy ion collision with variety of equation of state and study the formation of fragments. It will give us the possibility to check the role of different equations of state and momentum dependent interactions in multifragmentation.

Chapter 2

Methodology

2.1 Quantum Molecular Dynamics Models (QMD)

The QMD model[15] is a N-body theory which simulates heavy ion reaction at intermediate energies on an event by event basis. Here each event is simulated independent of other. Quantum molecular dynamics (QMD) model contains two dynamical ingredients, the density dependent mean field and the in-medium nucleon-nucleon cross-section. In this model each nucleon is represented by a coherent state and has Gaussian-shaped density distribution. The model mainly consist of three steps, which are as following:

1. Initialization

2. Propagation

3. Collision

Firstly we have to generate the nuclei, this procedure is called initialization. These nucleons then propagate under the influence of surrounding mean field. This is termed as propagation. Finally the nucleons are bound to collide if they come too close to each other; this part is called as collision[15].

In order to explain experimental results much better, the original version of QMD was modified to include isospin degree of freedom explicitly and the isospin dependence as for the coulomb potential, symmetry potential, N-N cross-sections and Pauli blocking, which is known as Isospin-dependent Quantum molecular dynamics model (IQMD)[1]. Isospin dependent effect such as symmetry energy and isospin dependent cross-sections has been taken into account in intermediate energy heavy ion collisions. The best suited method to study isospin effects is the Isospin-dependent Quantum molecular dynamics.

2.2 Isospin Quantum Molecular Dynamics Model (IQMD)

The IQMD model [1] can explicitly represent the many-body states of the system and contains correlation effects to all orders and fluctuations. The best suited method to study isospin effects is the Isospin-dependent Quantum Molecular Dynamics (IQMD). The isospin-dependent quantum molecular dynamics (IQMD) [1] model treats different charge states of nucleons, deltas and pions explicitly [29]. The IQMD model has been used successfully for the analysis of large number of observables from low to relativistic energies[1,29]**.** The isospin degree of freedom enters into the calculations via both cross-sections and mean field. It has basically two advantages:

(1) Many-body process, in particular, the formation of complex fragments is treated.

(2) The model allows an event-by-event analysis of heavy ion reaction.

In order to describe the isospin effects of the dynamical process of HIC, quantum molecular dynamics (QMD) should be modified properly:

(1) The density dependent mean field should contain the correct isospin-dependent terms including symmetry potential and Coulomb potential.

(2) The in-medium N-N cross section should be different for neutron- neutron (proton-proton) and neutron-proton collisions, and finally.

(3) Pauli blocking should be counted by distinguishing neutron and proton.

This model also includes three important steps: First, one has to generate the nuclei. This procedure is called as initialization. Then propagate under the influence of surrounding mean field. This is termed as propagation. Finally, nucleons are bound to collide if they come too close to each other. This part is dubbed as collisions. The elastic and inelastic cross-sections for proton-proton, neutron-neutron as well as proton-neutron are supposed to be affected in the presence of isospin. In the following, we shall discuss all of these parts in detail.

2.3 Initialization

In this model the nucleons are represented by the Gaussian-shaped density distributions. Here the centroids of the Gaussians in the nucleus are randomly distributed in a phase space sphere ($r \leq R$ and $P \leq P_F$) with radius $R = 1.12A^{⅓}$ fermi in accordance with the liquid drop model. Each nucleon occupies a volume of h^3, so that phase space is uniformly filled. The Fermi momentum depends on the ground state density. For $\rho_0 = 0.17fm^{-3}$ the value of P_F ~268MeV/c. Due to this, nucleon close to the surface (where the local potential energy is low) are unbounded initially. As a result binding energy is low as compared to the Weizsacker mass formula i.e there is reduced binding energy per nucleon as compared to Weizsacker mass formula. Hence, the initialized nuclei are less stable against spurious particle evaporation as compared to QMD model.

Finally, it should be noted that IQMD performs a Lorentz contraction of the nucleus coordinate distribution which is not present in QMD and also important for high energies. Interaction range Gaussian width is regarded as a description of the interaction range of a particle. Its influence disappears for infinite nuclear matter, whereas, for finite systems it plays an important role. It is denoted by L. The interaction range parameter L influences the interaction density for finite system.

In IQMD, the Gaussian width can be used as an optional input parameter. The system dependence of parameter L in IQMD has been introduced in order to obtain maximum stability of the nucleonic density profiles. As an example, for Au+Au a value of $L = 8.66fm^2$ is chosen, for Ca+ Ca and lighter system $L = 4.33fm^2$.

2.4 Propagation

The successfully initialized nuclei are then boosted towards each other with a proper center of mass velocity using relativistic kinematics. The nucleons of target and projectile interact via two and three body Skyrme forces and the Yukawa potential. The isospin degree of freedom is treated explicitly by employing a symmetry potential and explicit Coulomb forces

between the protons of colliding target and projectile. All this provide us a correct distribution of protons and neutrons within the nucleus.

The Hamilton equations of motion for the propagation of hadrons are:

$$\frac{dr_i}{dt} = \frac{d\langle H\rangle}{d\, p_i}; \tag{2.1}$$

$$\frac{dp_i}{dt} = -\frac{d\langle H\rangle}{d\, r_i} \tag{2.2}$$

2.5 Potentials used in IQMD

The IQMD-model offers rather stable density distributions and good energy conservation, however for the price of nucleon evaporation and improper binding energies (E_{Bind}~ 4-5 MeV/nucleon for heavy nuclei instead of 8 MeV/nucleon).

The Hamiltonian function <H> contains all the possible interactions of the particles of the system. The total Weigner density is therefore, sum of all nucleons. The expectation value of the Hamiltonian is i.e a total Hamiltonian function with a kinetic energy T and a potential energy V is given by

$$\langle H\rangle = \langle T\rangle + \langle V\rangle$$

$$= \sum_i \frac{{p_i}^2}{2m_i} + \sum_i \sum_{j>i} \int f_i(\vec{r},\vec{p},t) V^{ij}\left(\overrightarrow{r'},\vec{r}\right) \times f_j(\overrightarrow{r'},\overrightarrow{p'},t)\, d\vec{r}\, d\vec{r}'\, d\vec{p}\, d\vec{p}' \tag{2.3}$$

The potential in above equation′s is the sum of the following specific elementary potentials

$$V = V_{Sky} + V_{Yuk} + V_{Coul} + V_{mdi} + V_{sym}$$

With a local hard core repulsion,

$$V_{loc} = \sum_i \sum_{j>i} t_1 \delta(\vec{r}_i - \vec{r}_j)$$

$$+ \sum_i \sum_{j>i} \sum_{k>j} t_2 \delta(\vec{r}_i - \vec{r}_j) \delta(\vec{r}_i - \vec{r}_k), \quad (2.4)$$

The Yukawa short-range term,

$$V_{Yuk} = \sum_i \sum_{j>i} t_3 \frac{\exp(|\vec{r}_i - \vec{r}_j|/\mu)}{(|\vec{r}_i - \vec{r}_j|/\mu)} \quad (2.5)$$

The Yukawa potential V_{Yuk} in IQMD is very short ranged and weak (= 0.4fm). Additional attractive Yukawa forces hence modify the EOS. Yukawa forces stabilize the nuclei because of the increase of the interaction range as compared to a δ-like Skyrme potential. Thus nucleons notice earlier that they will arrive at the surface and are more effectively deaccelerated without this potential. In addition the fluctuations are reduced.

The Coulomb term with only a mean value for the nucleon charge because in QMD the isospin of the particles is not included,

$$V_{coul} = \sum_i \sum_{j>i} \frac{Z_i Z_j e^2}{|\vec{r}' - \vec{r}|} \quad (2.6)$$

And the momentum dependent interaction

$$V_{mdi} = \sum_i \sum_{j>i} t_4 \ln(1 + t_5(\vec{p}_i - \vec{p}_j)^2) \delta(\vec{r}_i - \vec{r}_j) \quad (2.7)$$

In addition to the potential used in QMD, a symmetry potential between protons and neutrons corresponding to the Bethe-Weizsacker mass formula has been included

$$V_{Sym}^{ij} = t_6 \frac{1}{\rho_o} T_3^i T_3^j \delta(\vec{r}_i' - \vec{r}_j) \quad (2.8)$$

Where T^{i}_{3} and T^{j}_{3} denote the isospin projection of particles i and j. Other baryonic potentials like V^{ij}_{sym} and V_{mdi} are defined isospin-independent like in all other flavors. The parameters are propagated under the total interaction calculated by the Hamiltonian equations of motion (2.1) and (2.2).

Parameters used in equations (2.5) to (2.8) are shown in table below:

IQMD parameters	
t_3	15 MeV
t_4	1.57 MeV
t_5	5.10^{-4} MeV^{-2}
t_6	25 MeV
μ	0.4 fm

Table 2.1: IQMD parameters used in equation (2.5) to (2.8)

2.6 Collision

Two particles collide if their minimum distance d, i.e. the minimum relative distance of the centroids of the Gaussians during their motion, in their CM frame fulfills the requirement:

$$|r_i - r_j| \leq \sqrt{\frac{\sigma_{tot}}{\pi}} \ , \sigma_{tot} = \sigma(\sqrt{s}, type), \qquad (2.9)$$

Where the cross-section is assumed to be the free cross section of the regarded collision type ($N - N$, $N - \Delta$...). The total cross-section is the sum of the elastic cross -section and all inelastic cross-sections. The main processes include:

$$\text{Elastic}\begin{cases} N+N \rightarrow N+N & (a) \\ N+\Delta \rightarrow N+\Delta & (b) \\ \Delta+\Delta \rightarrow \Delta+\Delta & (c) \end{cases}$$

$$\text{Inelastic}\begin{cases} N+N \rightarrow N+\Delta & (d) \\ N+\Delta \rightarrow N+N & (e) \end{cases}$$

Experimental cross sections are used for the processes *(a)* and *(d)*. The cross section for *(e)* is obtained by the detailed balance method. The cross section for processes *(b)* and *(c)* are taken to be same as that of process *(a).*

In addition to this the Pauli blocking of baryons is also taken into account by checking the phase space densities in the final state. The final phase space fractions P_i and P_j, which are already occupied by other nucleons, are determined for each of the scattering baryons. For each collision the phase space densities in the final state are checked in order to assure that the final distribution in phase space is in agreement with the Pauli principle ($P \leq 1$). The collision is then blocked with a possibility

$$P_{block} = 1-(1-P_i)(1-P_j) \qquad (2.10)$$

Where P_i and P_j are the already occupied phase space fractions by other nucleons.

2.7 Methods of clusterization

Minimum spanning tree method (MST)

In MST [30], two nucleons share the same fragment if their centroids are closer than a distance d_{min},

$$\left|\vec{r}_i - \vec{r}_j\right| \leq d_{min}$$

Where r_i and r_j are the spatial positions of both nucleons. The minimum distance d_{min} has been used as a free parameter which varies between 2 fm - 4 fm. Its influence on multifragmentation (at 200-300 fm/c) is reported to be small. This approach (being a spatial

distance approach) cannot detect different fragments which are almost overlapping and therefore, will give a single big fragment during the early stage of the reaction where density is quite high and the interactions among the nucleons are still active. In other words, the simple coordinate space approach cannot address the question of time scale of the fragments. To study the time of fragment formation, one needs to derive a method which should be able to detect the overlapping fragments. In the present thesis we shall vary the distance between the nucleon between 2 and 6 fm at fixed momentum constraint. This will give us proper value of d_{min} which can give us most bound configuration. Here we want to optimize the value of $d_{min.}$

Chapter 3

Spatial Correlations

3.1 Introduction

Our main interest is to optimize the value of distance between nucleon to form cluster. Finally obtained method should be fast, accurate and applicable to whole mass range in periodic table. Here we plan to vary the distance between the nucleon from minimum to maximum at fixed momentum constraints. Also fragments formed by putting constraint in space.

3.2 Phase Space Analysis

A plot of position and momentum variables as a function of time is sometimes called a phase plot or a phase diagram. Phase diagram, however is more usually reserved in the physical sciences for a diagram showing the various regions of stability of the thermodynamic phases of a system. fig.3.1 and fig.3.2 the phase space of nucleons for X-Z and $P_x - P_z$ plane for the reaction of $_{79}Au^{197}$ + $_{79}Au^{197}$ at semi-peripheral geometry. The panels from top to bottom are representing the position of nucleons of projectile and target at different times, while right and left panels are for Soft momentum dependent (SMD) equation of state and Soft EOS respectively. The phase space remains unaffected by the momentum dependent interactions until the projectile and target overlap with each other. During and after the overlapping (above, t = 30fm/c), more repulsion is observed in the projectile as well as target nucleons in X-Z as well as $P_x - P_z$ plane. Moreover, more radial expansion of the matter is observed in the presence of momentum dependent interactions in the reaction plane. The momentum dependence of the nuclear equation of state has been reported to affect the collective flow and particle production drastically [15]. Some initial investigations also point toward its important role in multifragmentation [31,32]. Due to the repulsive nature of SMD EOS, propagating nuclei are reported to emit nucleons and light complex fragments. We also keep in the mind that the response of momentum

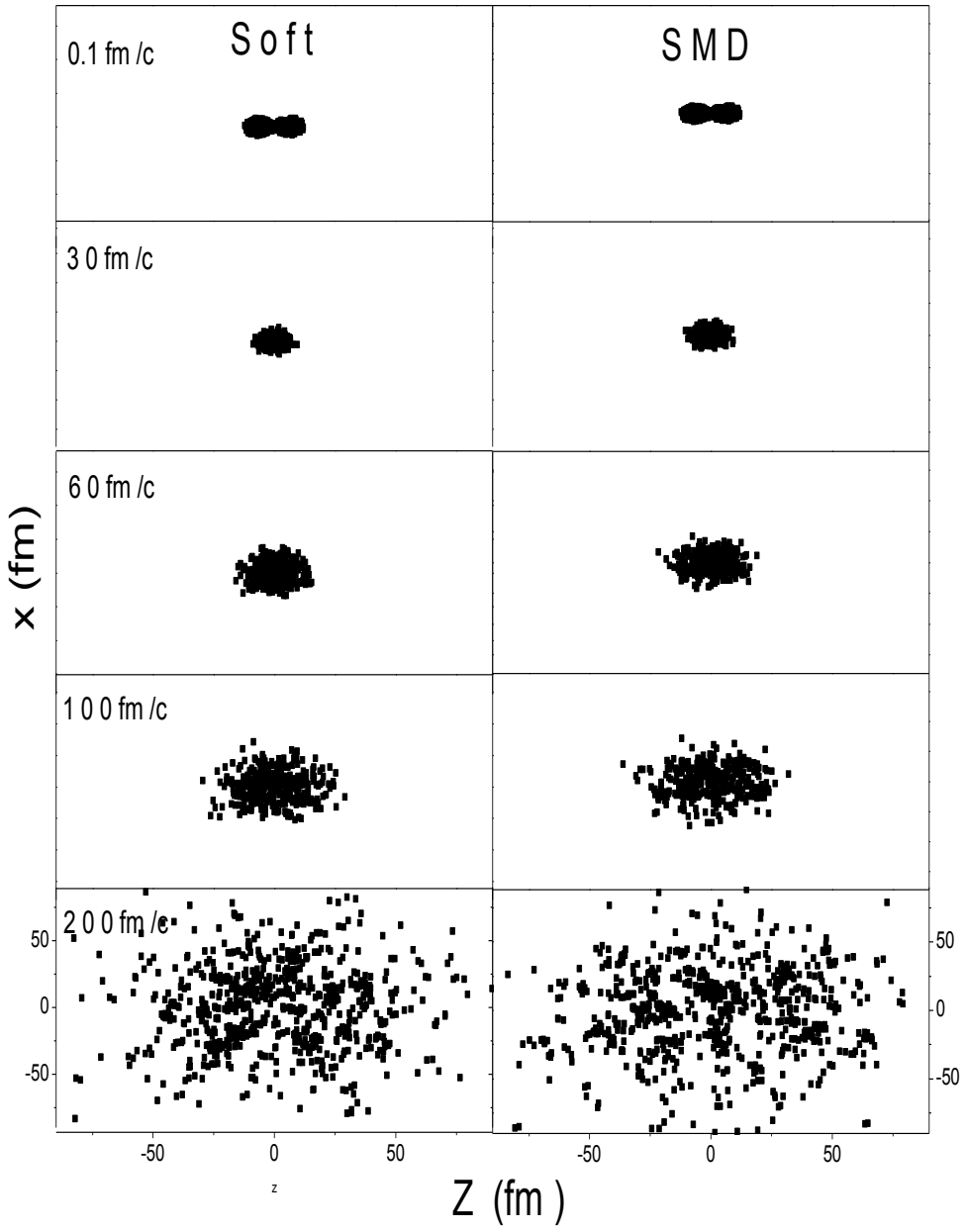

Fig.3.1. Phase space distribution of the projectile and target nucleons without (left) and with momentum dependent interactions (right) in X-Z plane. The reaction under study is $_{79}Au^{197}$ + $_{79}Au^{197}$ at incident energy E = 100 MeV/nucleon for semi-peripheral geometry. The panels from top to bottom are representing the positions at different times.

dependent interactions also depend on the system size. Therefore more is the repulsion, more is the squeeze-out of the particles and more is the transfer of the momentum in the radial direction as shown in $P_x - P_z$ graph and hence more over more scattering in phase space.

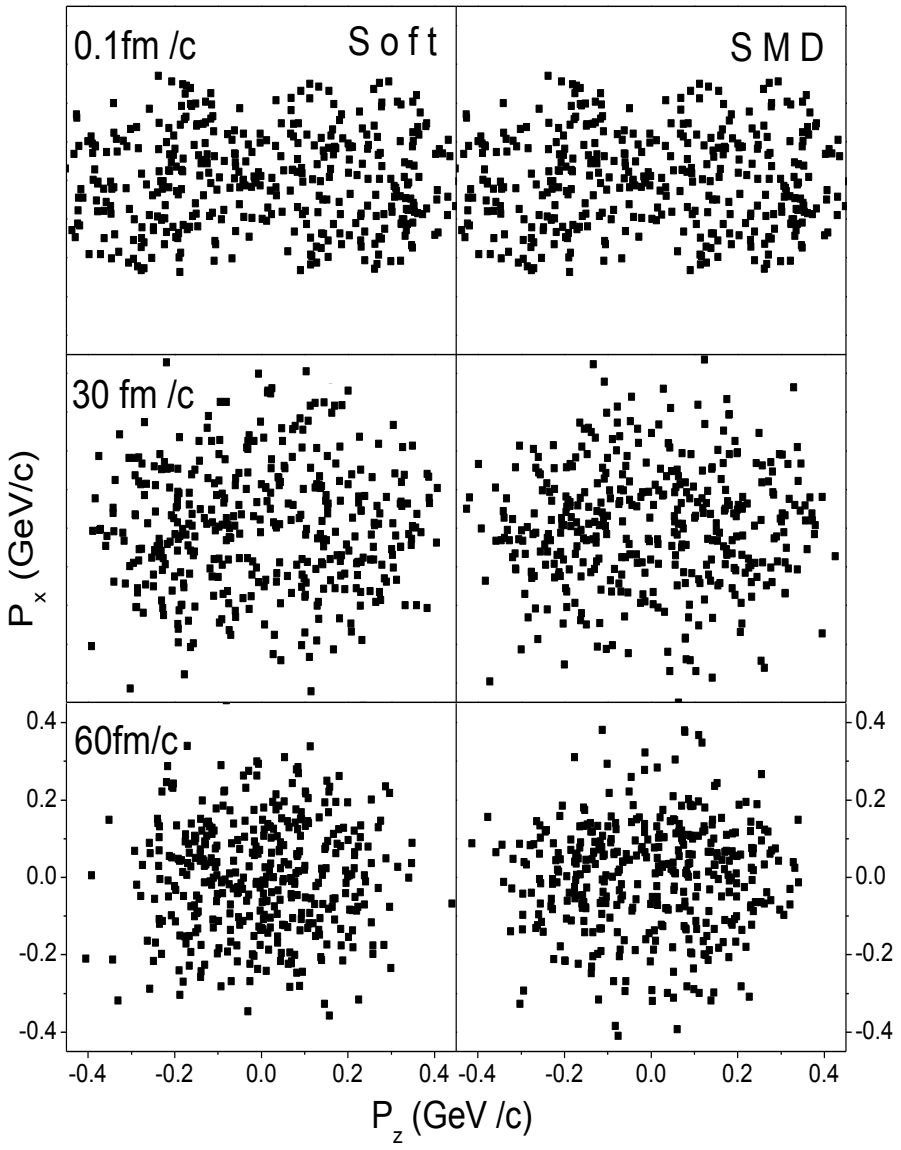

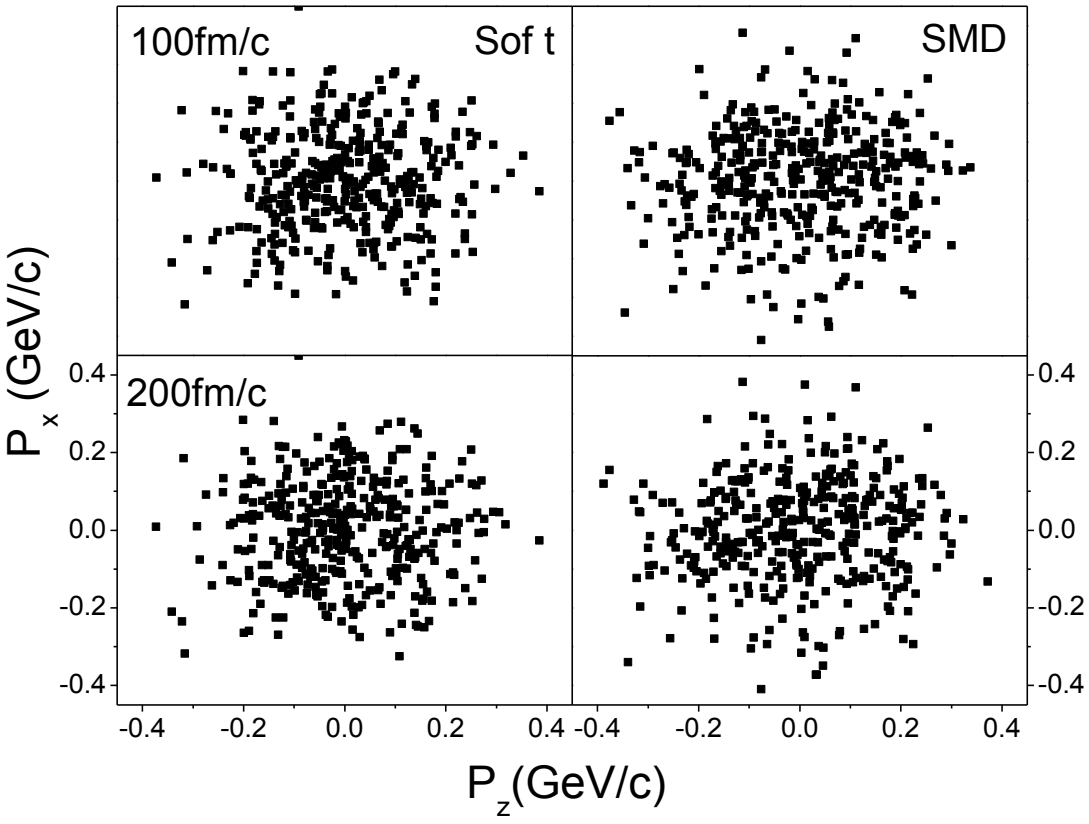

Fig.3.2. Momentum phase space distribution of the projectile and target nucleons without (left) and with momentum dependent interactions (right) in P_X-P_Z plane. The reaction under study is $_{79}Au^{197}$ + $_{79}Au^{197}$ at incident energy E = 100 MeV/nucleon for semi-peripheral geometry. The panels from top to bottom are representing the positions at different times.

3.3 Time evolution of nucleon- nucleon collision

In fig.3.3. we display the time evolution of the allowed collision at incident energies of 100 MeV/nucleon for two colliding geometries corresponding to b = 0 and b = 0.6. It has been observed that collision rate depend upon the participant zone and incident energy. At semi-peripheral geometries, the participant zone decreases and hence decrease is observed in

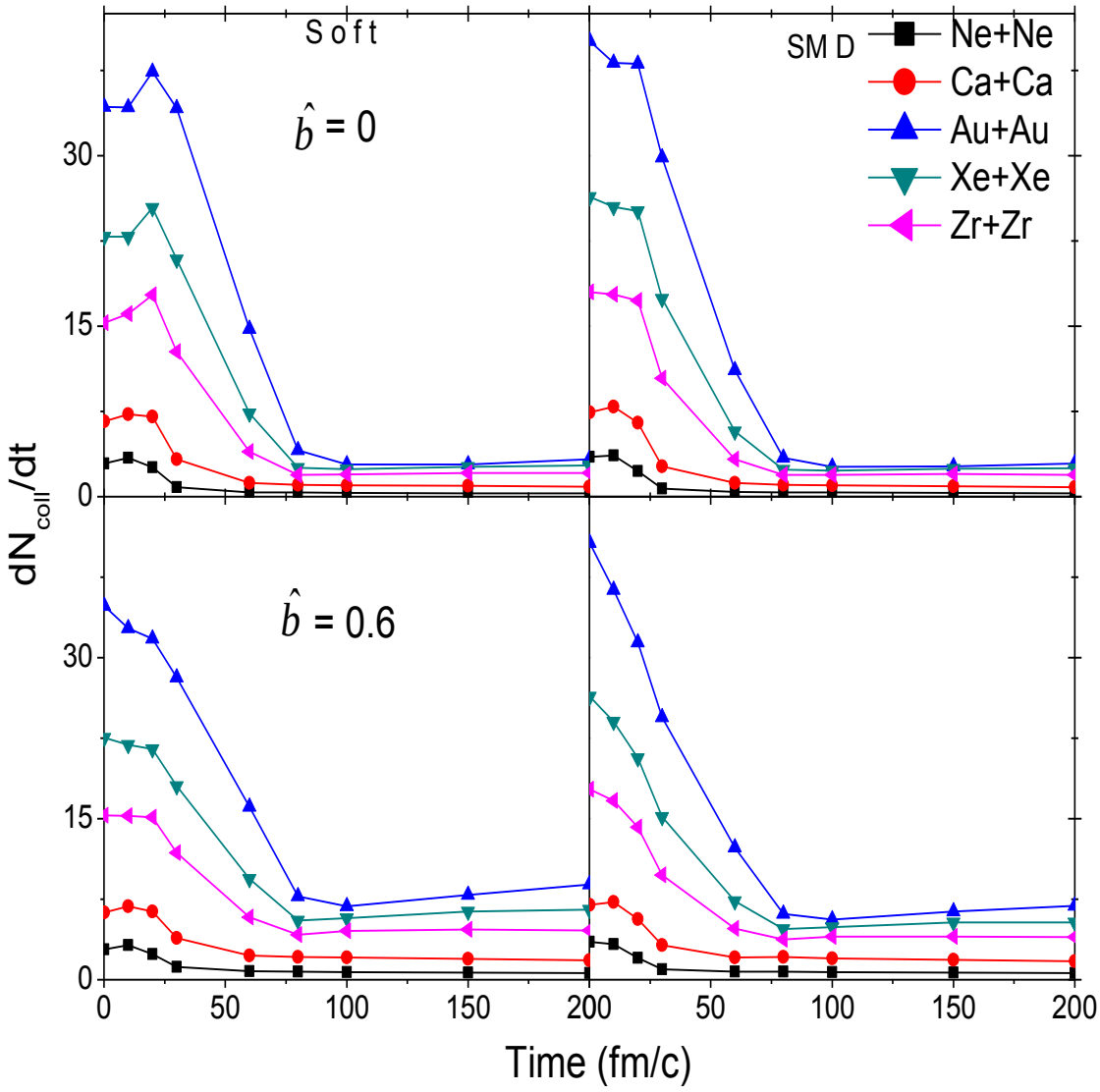

Fig: 3.3 Allowed collision as a function of the time. The top and bottom panel represents the reaction at 100 MeV/nucleon. The top and bottom panel represent, respectively, the central collision b = 0 and peripheral collision b = 0.6. The left panel represent the reaction for soft EOS and right panel represent reaction for SMD EOS.

the number of collisions at low as well as high incident energies compared to central geometries. As the incident energy increase, collision rate is found to increase with the probability of breakup of initial correlations among the nucleons. However, the momentum dependent interactions are found to suppress the number of collisions at all incident energies as well as at all impact parameters.

3.4 Time evolution of Free nucleons

In fig.3.4 and fig.3.5 we have displayed the time evolution of free nucleon with and without momentum dependent interactions for different systems at central collision and at incident energies 100 MeV/nucleon. Here we have varied the distance between the nucleon from R_{clus}= 2 fm to R_{clus}= 6 fm minimum to maximum at fixed momentum constraints. From the two figure of free nucleon it is clear that enhanced production of F.N's takes place in the presence of momentum dependent interactions as compared to static one. This is due to the repulsive nature of the MDI's, which helps in breaking the heavier fragments into FN's. If we keep the value of R_{clus}= 2 fm then we obtain maximum no. of free nucleon for all the colliding nuclei, because 2 fm is very small range to keep the nucleon in same fragment. Clear systematic can be seen with increasing of R_{clus}. More and more nucleon get bounded in the fragments and hence decrease in the production of free nucleon. Moreover, the behavior of increase in multiplicity of fragments with the size of the system is observed in the presence of static as well as momentum dependent interactions.

3.5 Time evolution of light mass fragments

In fig.3.6, we have displayed the time evolution of light mass fragments for different systems for central collision and at incident energies 100 MeV/nucleon. Here we varied the distance between the nucleon from 2 fm to 6 fm. These fragments are formed during the collision at central geometry, with soft equation of state and at energy 100 MeV/nucleon. It can be seen from the figure that the trend for light mass fragments is same as for the free nucleons. At the start of the reaction a minimal number of LMF's are produced but as the time increases the

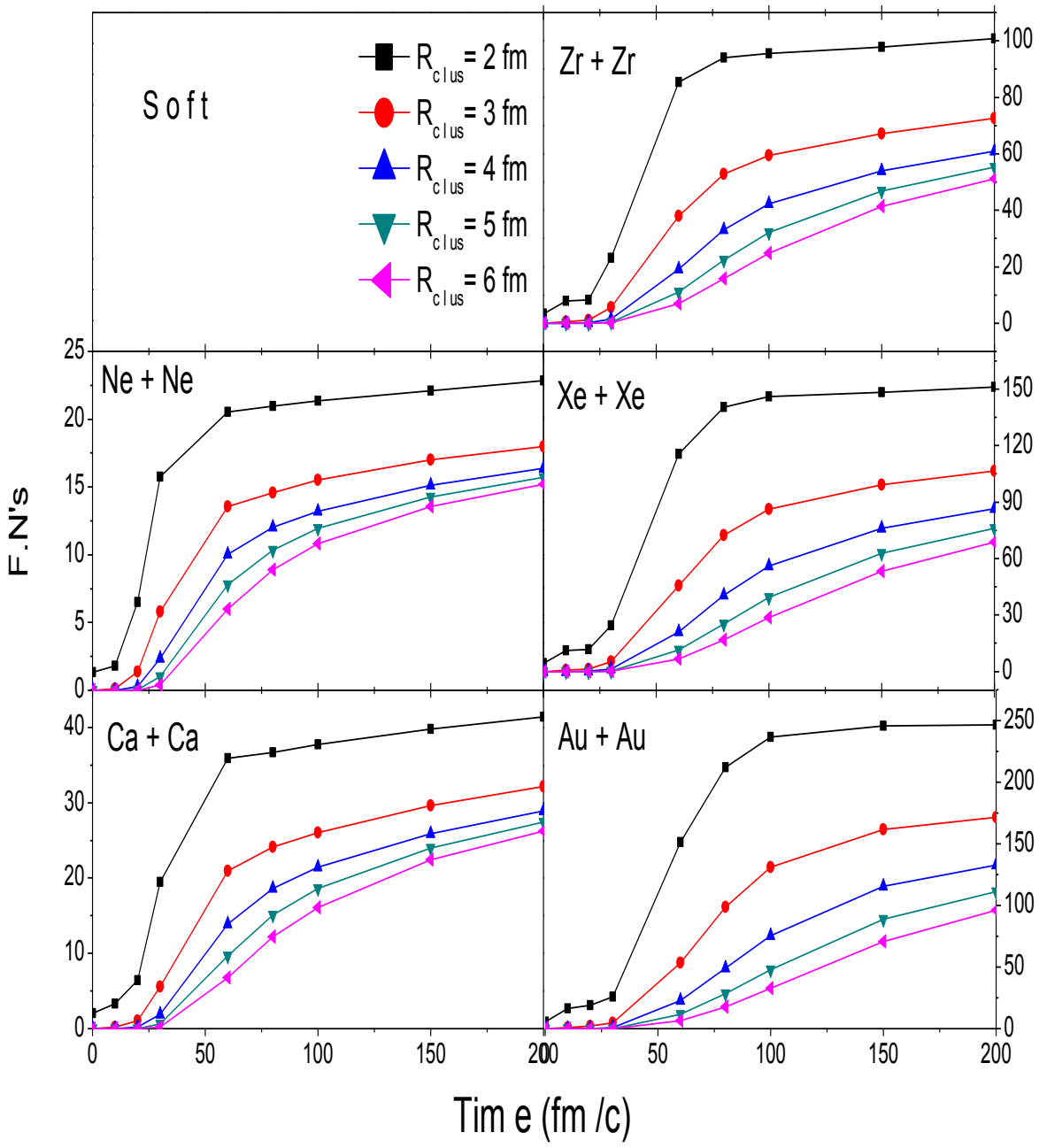

Fig.3.4. Multiplicity of free nucleon (A =1) for central collision for Soft EOS.

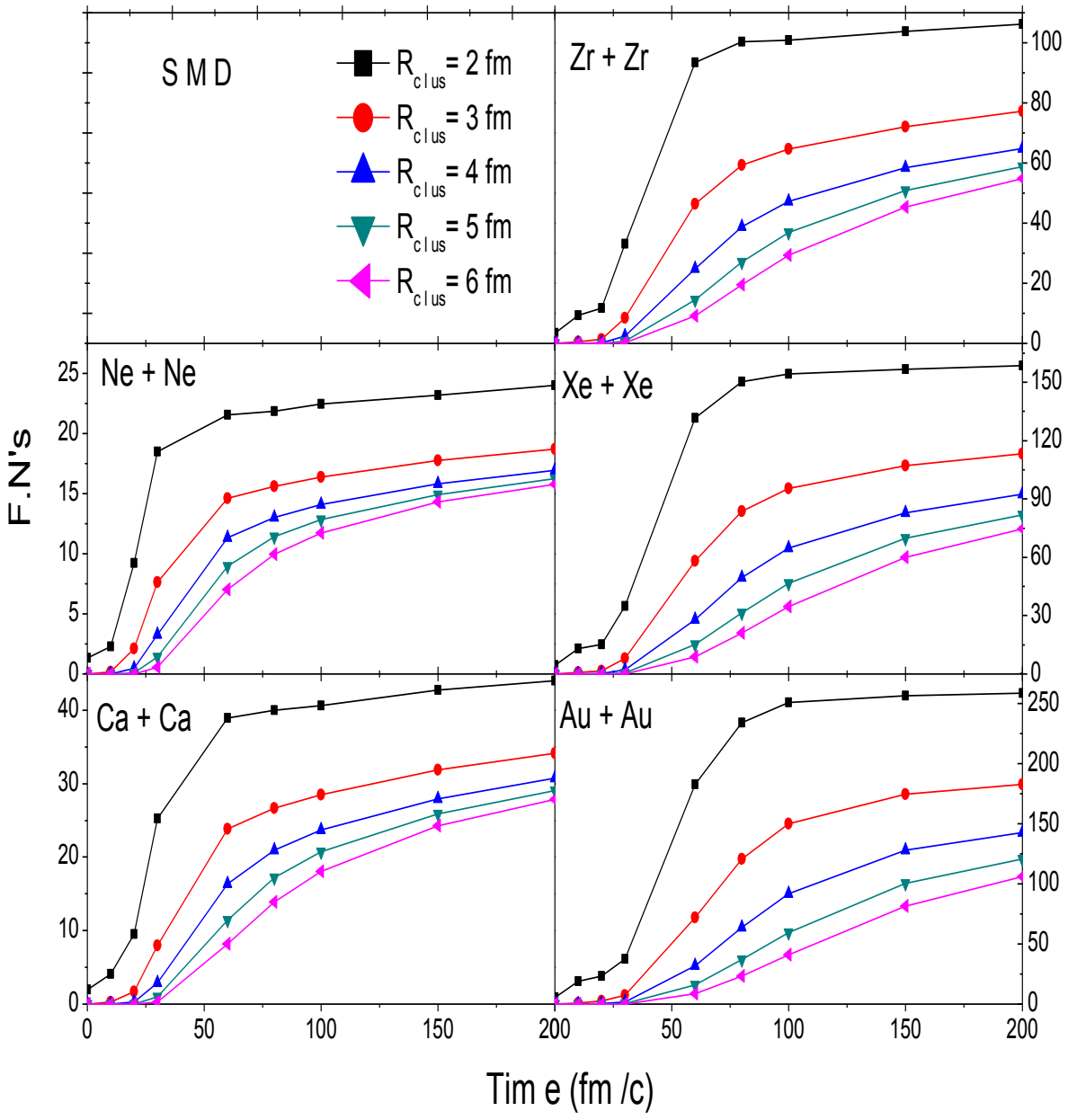

Fig.3.5. Multiplicity of free nucleon (A=1) at central collision for SMD EOS.

number of light mass fragments goes on increasing. But when t=200fm/c the production of LMF's became nearly same for all values of R_{clus}. Also the distance between the nucleon varied so, when the distance between the nucleon decreases, the repulsion between the nucleons increases which enhance the production of LMF's while increasing distance between nucleon, decrease the production of LMF's. Moreover, from the figure we observed that multiplicity of LMF's increases with increase in the size of the system. For large nuclei large number of LMF's are produced as compare to small nuclei.

3.6 Variation of various fragments with space correlation

In this section, we have display the variation of multiplicity of various fragments for different value of R_{clus} with and without momentum dependent interaction (SMD) at incident energy 100 MeV/nucleon for different system of nuclei. In fig.3.7, we display the variation of free nucleon as function of R_{clus}. The values are taken at 200fm/c. The fragments formed at time 200 fm/c (typical saturation time) have been taken for the present analysis. The production of free nucleons depend upon the distance between the nucleon. When the distance between the nucleon is small (say 2 fm), maximum number of free nucleon are produced. The production of free nucleon also depend upon the size of nuclei, as the size of nuclei increases production of free nucleons increases as it clear from the fig.3.7. for $^{197}Au_{79}+^{197}Au_{79}$ the production of free nucleon is more as compare to $^{20}Ne_{10}+^{20}Ne_{10}$ and $^{131}Xe_{54}+^{131}Xe_{54}$. Due to repulsive nature of momentum dependent interaction the phase space is more scattered hence low value of R_{clus} give more free nucleon as compare to static equation of state case. The fig.3.8 is same as fig.3.7 but for light mass fragments ($2 \leq A \leq 4$). As the distance between the nucleon increases, destruction also increases which increase the production of LMF's. If we take the value of R_{clus} = 4 fm then we obtain the maximum no. of LMF's for all the colliding nuclei. Also the production of LMF's depend upon the size of colliding nuclei, for large nuclei, more no. of LMF's produced as compare to small nuclei. From the figure it is clear that enhanced production of LMF's take place in the presence of momentum dependent interaction as compare to static one. This is due to repulsive nature of the MDI's, which help in breaking the heavier fragments into LMF's. Moreover, the behavior of increase in multiplicity of fragments with the size of the system is observed in the presence of static as well as

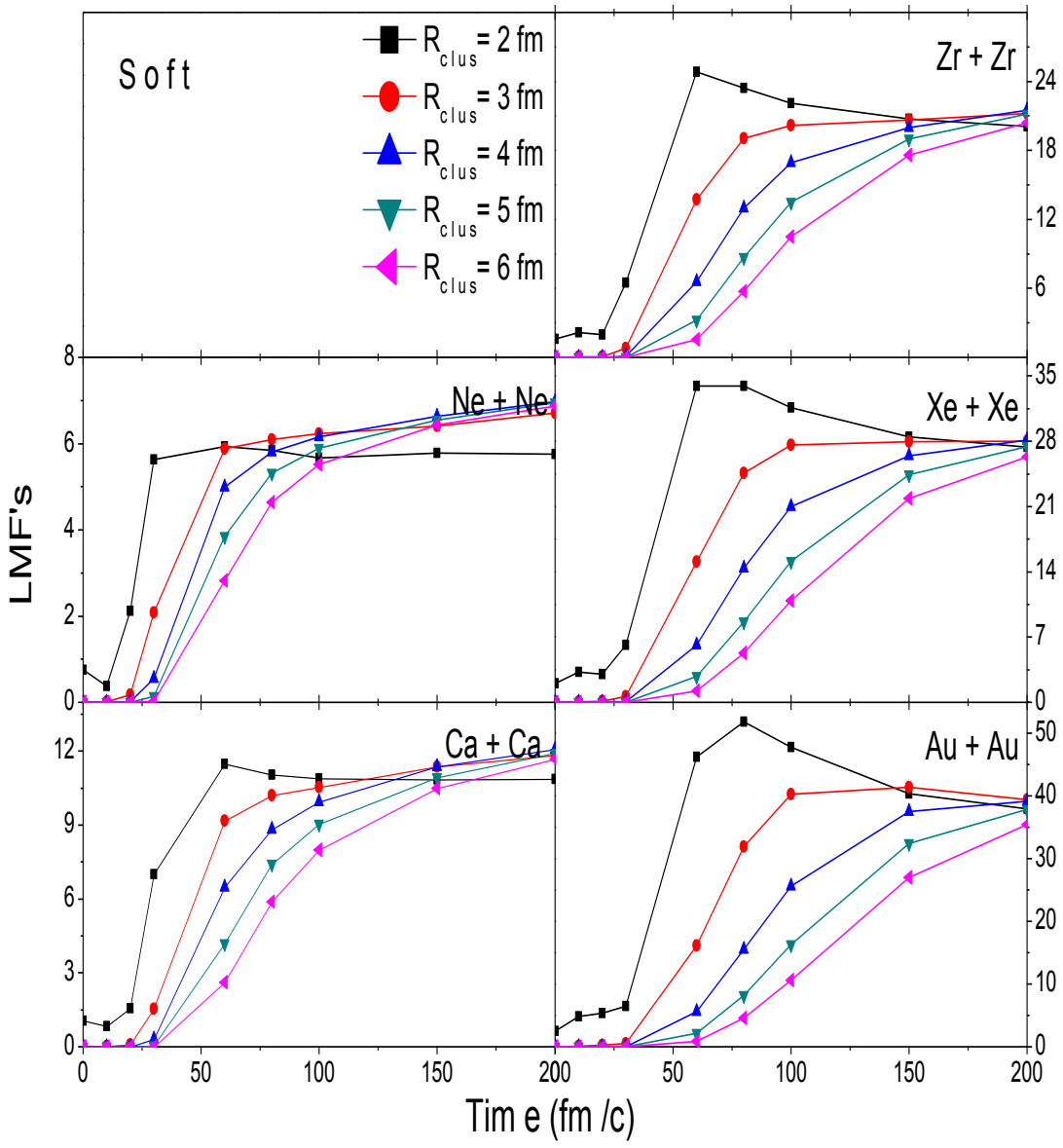

Fig.3.6. Multiplicity of light mass fragments (2<*A*<4) at central collision for Soft EOS.

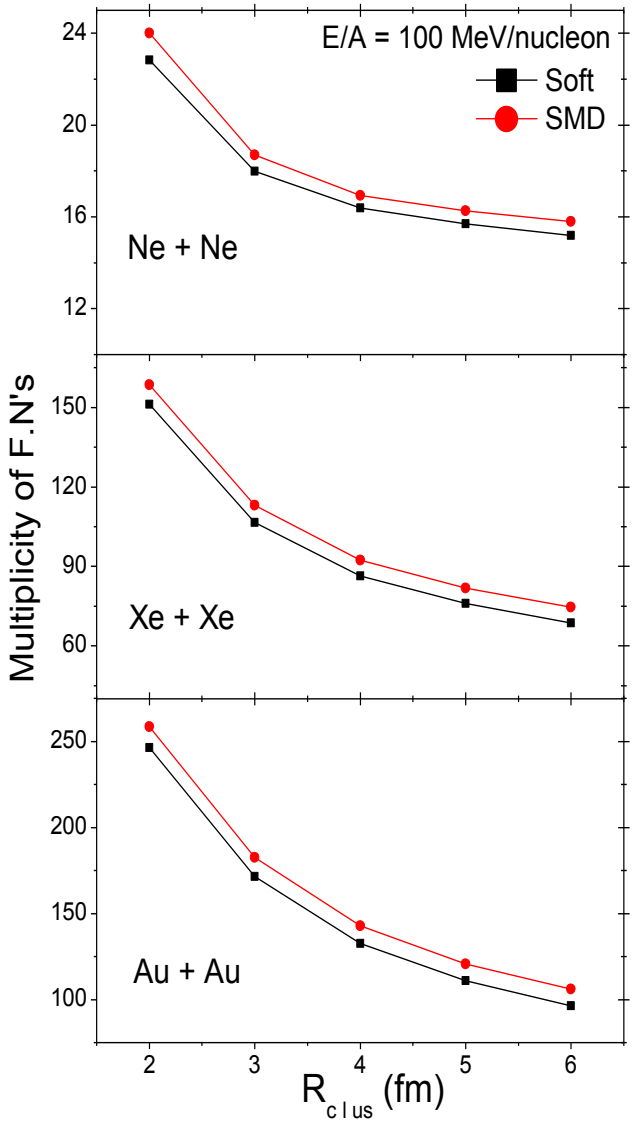

Fig.3.7. Variation of Multiplicity of free nucleon as function of R_{clus} (fm) for central collision.

momentum dependent interactions. One can conclude that maximum production of LMF's take place at 4 fm.

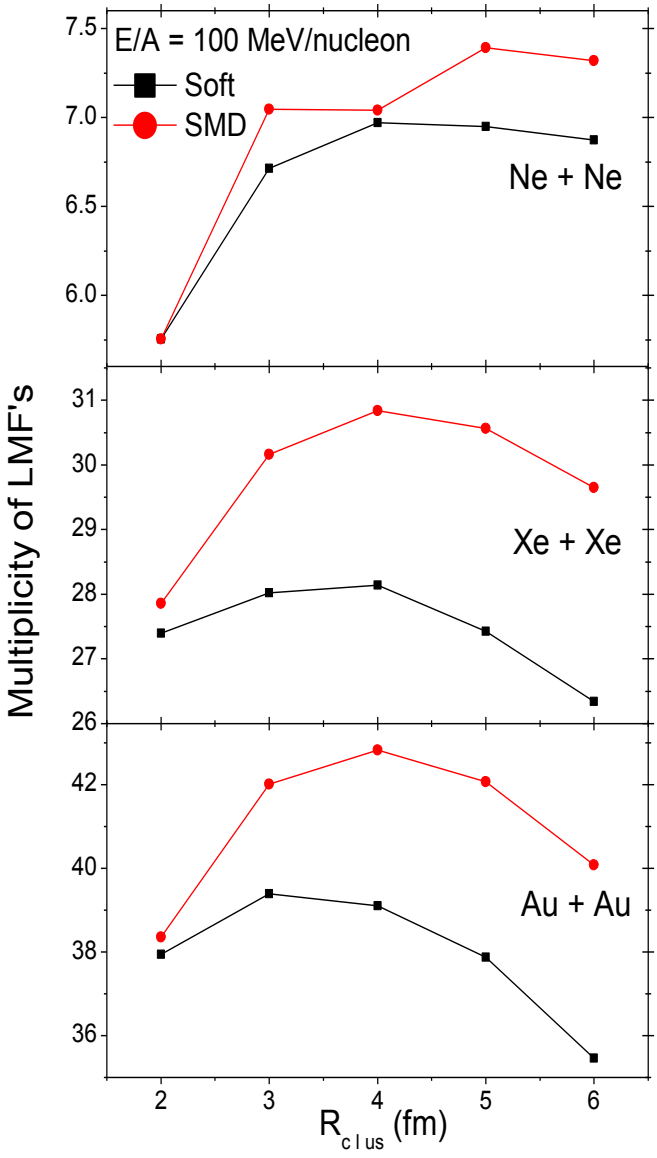

Fig.3.8. Variation of multiplicity of LMF's as function of R_{clus}(fm) for central collision.

In the Fig.3.9 the variation in the production of intermediate mass fragments ($5 \leq A \leq A_{tot/6}$) as function of R_{clus} has been displayed at the same conditions as the free nucleons and light mass fragments have been displayed in the fig.3.7 & fig.3.8 respectively. The IMF's have different story to tell in comparison to free nucleons and LMF's. As the distance between the nucleon increases, increases the production of IMF's. Therefore when the distance between the nucleon is 6 fm then more number of IMF's are produced. The clear indication of origin

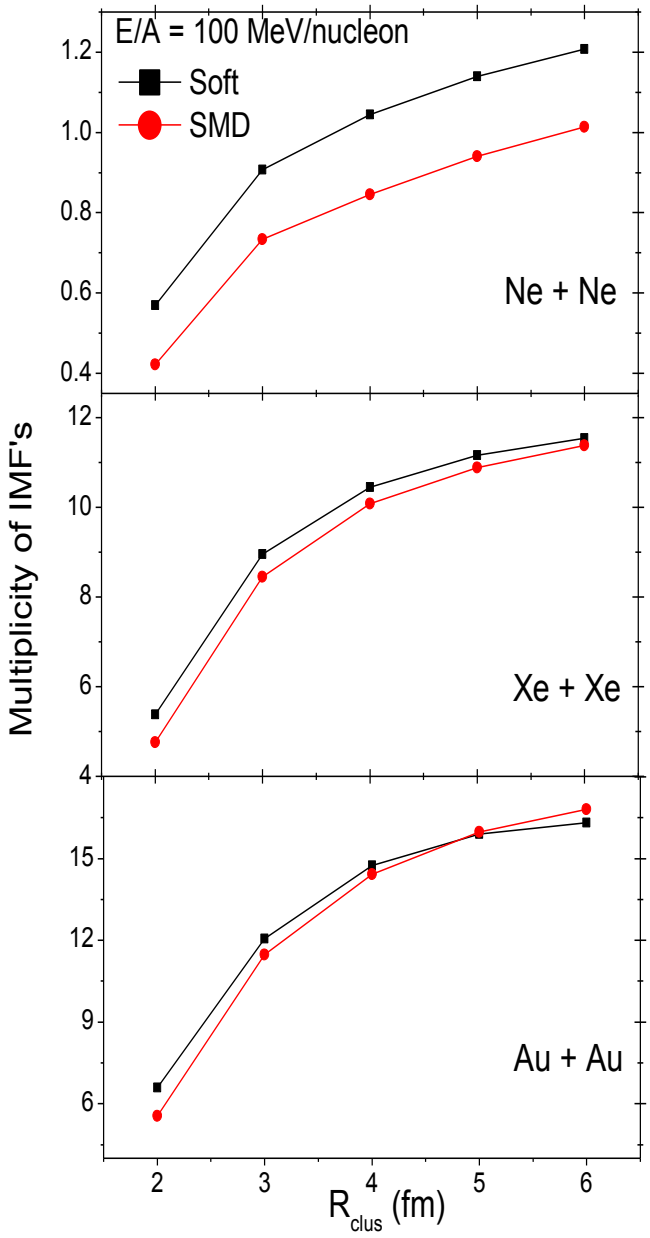

Fig.3.9. Variation of Multiplicity of IMF's as a function of R_{clus} (fm) for central collision.

for free & LMF's is from the participant zone, while for IMF's is from spectator zone. Hence low value of R_{clus} give less no IMF's. The production of IMF's also depend upon the size of nuclei, as the size of nuclei increases production of IMF's also increases as it clear from the

fig.3.6. for $^{197}Au_{79}+^{197}Au_{79}$ the production of IMF's is more as compare to $^{20}Ne_{10}+^{20}Ne_{10}$ and $^{131}Xe_{54}+^{131}Xe_{54}$. The fragments are found to be sensitive toward Soft and SMD equation of state. The production is more with soft as compared to SMD equation of state because SMD break the matter into small pieces as compared to Soft EOS.

We observe a delayed emission of all type of fragments using MST method which is due to the fact that the normal MST method depends on the spatial distance. Due to frequent nucleon-nucleon collisions in central collision geometry, an appreciable part of the nuclear matter is in the form of emitted nucleons and most of initial correlations among nucleons are destroyed which leads to the creation of unstable/unbound fragments. These fragments decay after a while and therefore, one has to follow the reaction dynamics for quite long time to obtain the stable and properly bound fragments. Lot of efforts have been made to avoid the creation of unbound/unstable/weakly bound fragments [33,34].

3.7 Multiplicity of IMF's with Scaled Impact Parameter

In fig.3.10, we display the multiplicity of IMF's with scaled impact parameter 0 and 0.6 at incident energy E=100MeV/nucleon. At central collision, more number of IMF's are observed. But as we go from central to semi central (b= 0.6), production of IMF's decreases. This is due to the low excitation energy, central collisions generate better repulsion and break the colliding nuclei into IMF's, whereas for the semi central collisions, the size of the fragment is close to the size of the reacting nuclei, therefore, one sees a very few IMF's. As clear from the fig.3.10 with increasing impact parameter the productions becomes smaller and smaller. The fig.3.10 shows the variation of multiplicity of IMF's and scaled impact parameter for SMD & Soft EOS. The enhanced production of IMF's take place in the presence of Soft EOS which break the heavier fragments into IMF's.

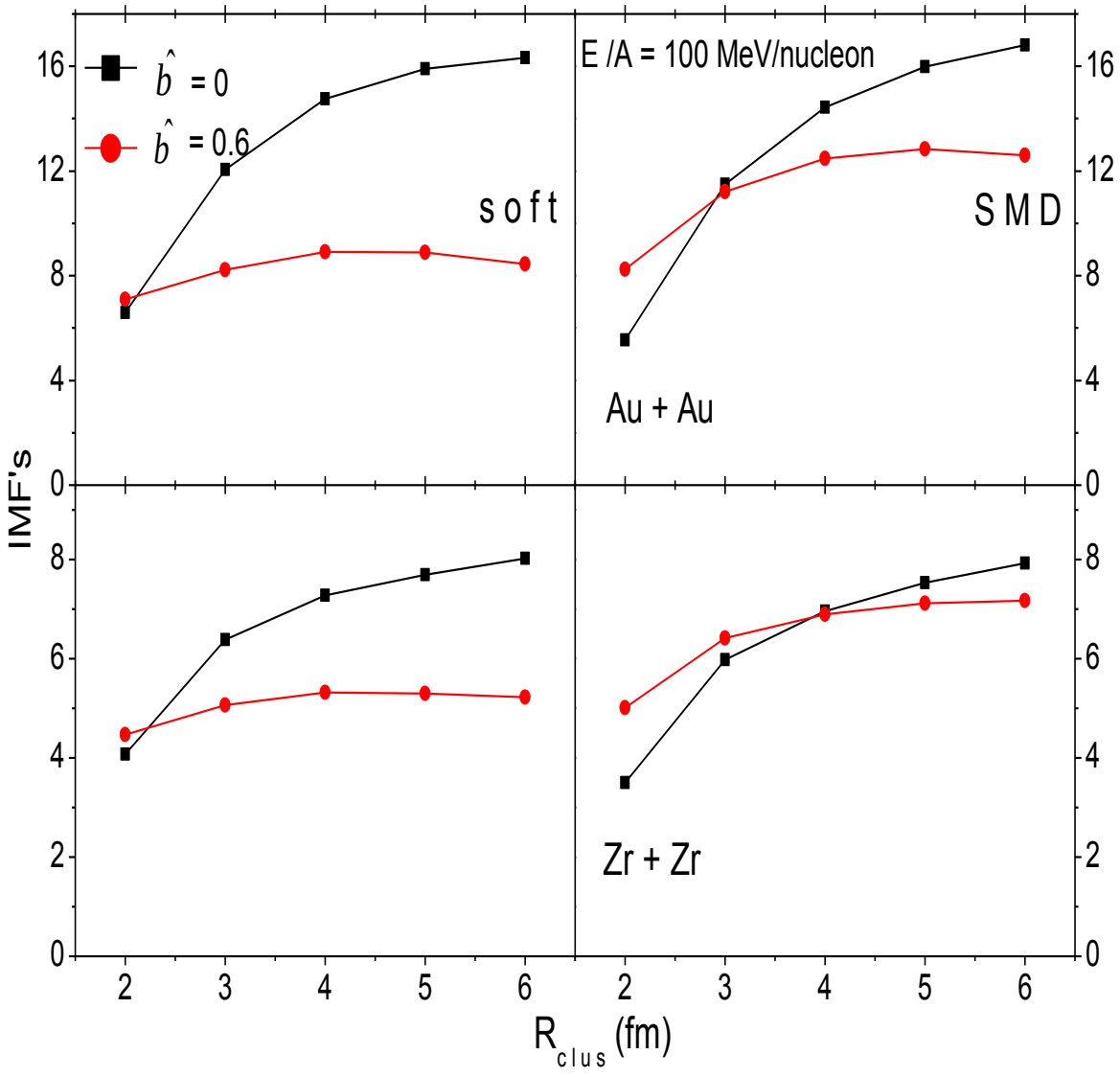

Fig.3.10. Multiplicity of IMF's of $^{197}Au_{79}$+$^{197}Au_{79}$ and $^{91}Zr_{40}$+$^{91}Zr_{40}$.

3.8 Energy dependence of the light mass fragments

The effect of different energies on fragmentation pattern is presented in fig.3.11. The collision of different nuclei at different energies ranging from 50 MeV/nucleon to 1000 MeV/nucleon is simulated at different impact parameters 0 and 0.3. Here, we display the multiplicity of light mass fragments as a function of energy and varied the distance between the nucleon from 3 fm, 4 fm and then 6 fm respectively. From the figure it is clear that the number of LMF's first increases as energy increases reaches a peak value at 200MeV/nucleon and then decreases as the energy increases. This trend is for symmetric systems i.e for $^{20}Ne_{10}$ +$^{20}Ne_{10}$, $^{40}Ca_{20}$ + $^{40}Ca_{20}$, $^{91}Zr_{40}$ +$^{91}Zr_{40}$, $^{131}Xe_{54}$ + $^{131}Xe_{54}$ and $^{197}Au_{79}$ + $^{197}Au_{79}$. It can be seen from the fig.3.11 that the number of light mass fragments formed are more for central collision as compared to semi-central collision. This is due to the reason that at central collision all the nucleons are taking part in the collision. The collision will be becoming more violent as the energy is increasing. As the energy is increasing, more compression zone will be there. The maximum number of LMF's will be produced at high energy due to more compression zone at high energy. Also with increase in energy Pauli blocking effect decreases. With the increase of energy, more number of clusters manage to qualify as light fragments. As the impact parameter increases, the production of light mass fragments drastically changes and they seems to falls linearly. It is seen that multiplicity of light mass fragments decrease with the increase in energy. The production of LMF's is highest at 200 MeV/nucleon which decreases with the increase in energy. Due to very small overlap at large impact parameter, the system does not receive enough energy and hence cools down after emitting few nucleons/LMF. Moreover, when the distance between the nucleon is maximum, more no. of LMF's produced. The production of LMF's is large for the case when the distance between the nucleon is maximum while small for smaller distance between the nucleon. Also with increase in the size of the system multiplicity of LMF's also increases as it clear from the figure. At very high energy complete destruction takes place and hence leads to less production of fragments.

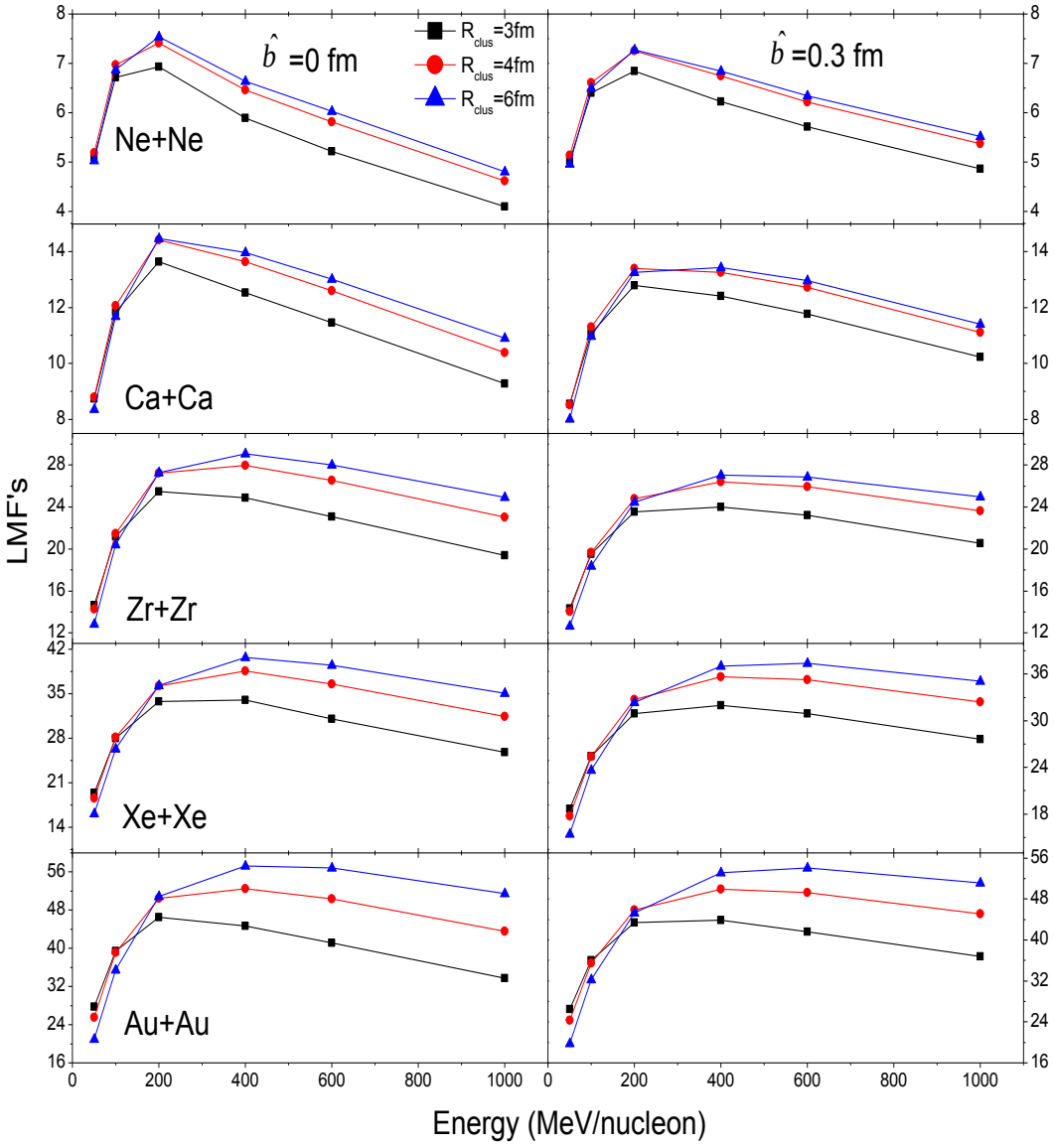

Fig.3.11.Multiplicity of light mass fragments as a function of energy at central and semi-central collision.

3.9 Energy dependence of the intermediate mass fragments

The fig.3.12. is same as the fig.3.11 but here we display the multiplicity of intermediate mass fragments as a function of energy. When a nucleus is excited to and beyond its total binding energy, it is predicted to decay into several IMF's. The multiplicity of intermediate mass fragments have been displayed for central collision and at semi-central collisions. The number of IMF's also first increases as energy increases reaches a peak value at 200MeV/nucleon and then decreases as the energy increases. Moreover the production of IMF's show rise and fall behavior with increase in energy which is in agreement with study carried out in Ref [35]. It can be seen from the fig.3.12 that the number of intermediate mass fragments formed more at semi-central collision as compared to central collision because destruction is less at semi-peripheral collision hence large number of IMF's are produced. Also the more number of IMF's are produced when the value of R_{clus} is large. From the figure it is clear that at distance 6 fm more IMF's are produced.

3.10 Dependence of various fragments on total mass of the system

In fig.3.13 the multiplicity of various fragments is displayed as a function of total mass of the system at incident energy 100 MeV/nucleon. The total mass of these reactions $^{20}Ne_{10}$ +$^{20}Ne_{10,}$ (40), $^{40}Ca_{20}$ + $^{40}Ca_{20}$ (80) , $^{91}Zr_{40}$ +$^{91}Zr_{40}$(182), $^{131}Xe_{54}$ + $^{131}Xe_{54}$(262) and $^{197}Au_{79}$ + $^{197}Au_{79}$(394) have been displayed. The values are taken at 200fm/c. It has been seen from the figure that the universal behavior of increase in multiplicity of LMF's with the size of the system is observed. With the increase in the size of system, number of the participant nucleons increases. This will lead to more thermalization of the system. Due to this reason, increase in multiplicity of LMF's will be observed, which will originate from the participant zone. But as the distance between the nucleon increases, the production of LMF's also decreases because as R_{clus} increases, more and more nucleon become a part of big fragment and hence leads to the production of more number of IMF's.

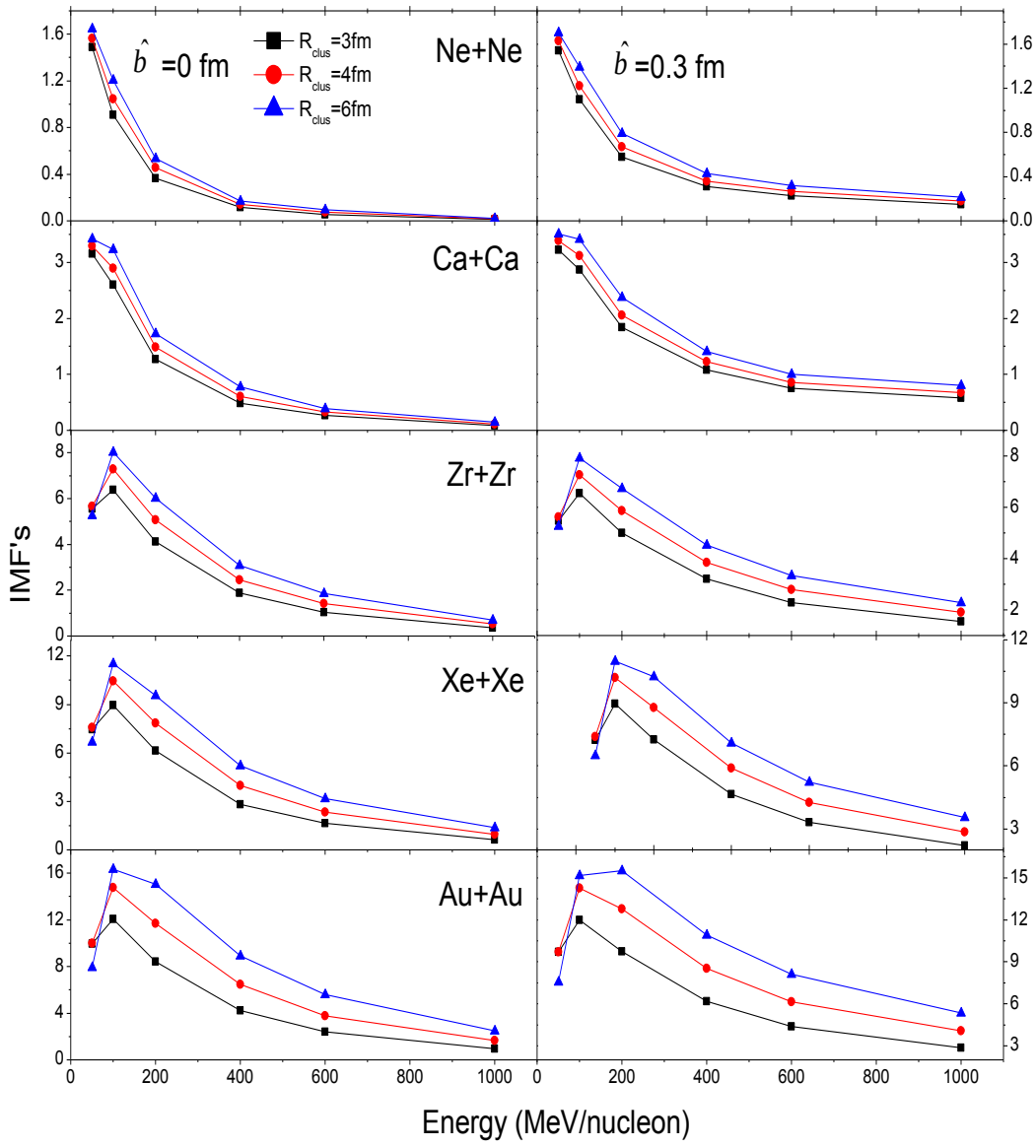

Fig.3.12.Multiplicity of intermediate mass fragments as a function of energy at central and semi-central collision.

But the intermediate mass fragments do not follow the same trend as followed by LMF's. The production of IMF's increases with the increases in mass number of the system as clear from the figure. But as the distance between the nucleon is increases, hence more number of IMF's are produced.

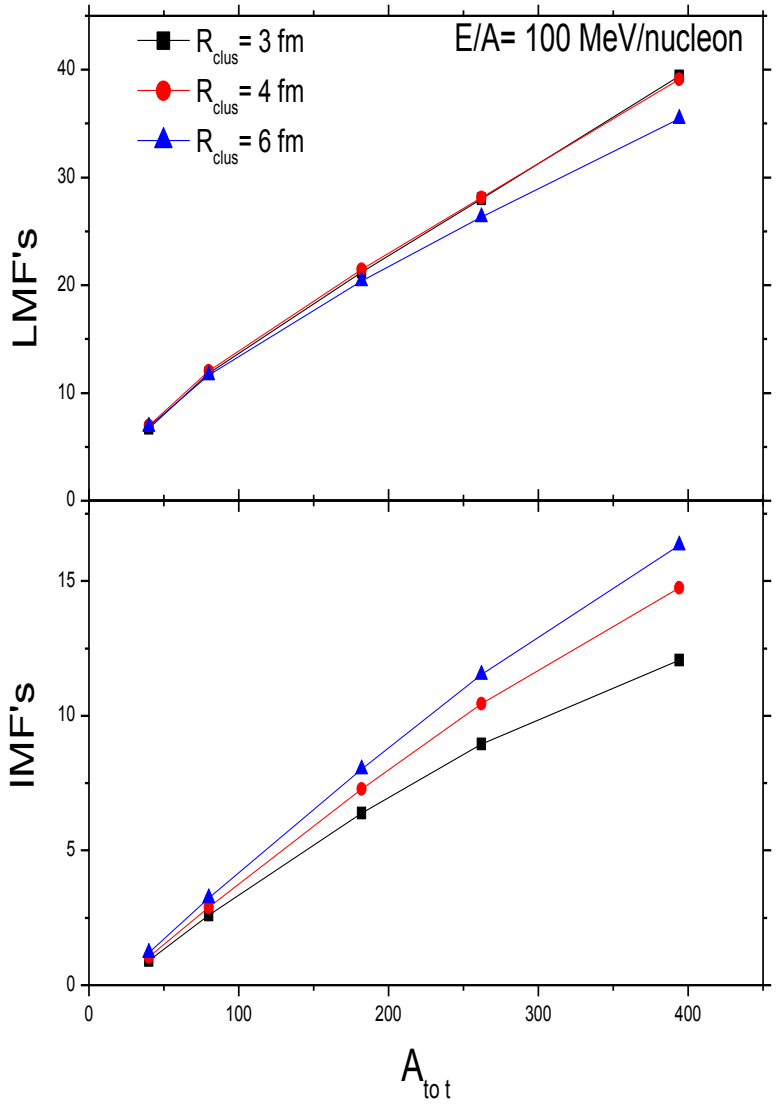

Fig.3.13. Multiplicity of LMF's & IMF's as a function of total mass of the system.

3.11 Comparison with experimental data

The ALADIN results are the most complete piece of data available for multifragmentation. In heavy ion collisions energy depositions covers the range of particle evaporation to multifragmentation emission and the total disassembly of the nuclear matter so called the '*rise and fall'* of multifragmentation [36]. The most prominent feature of the multifragment decay is the universality of the fragment and fragment charge correlation. Here we are comparing our results with experimental data of reactions $^{197}Au+^{197}Au$ at energy 600 MeV/nucleon [36]. In fig.3.14, we have shown IMF's as a function of Z_{bound} . The quantity Z_{bound} is defined as sum of all atomic numbers Zi of all projectile fragment with $Z_i > 2$. Here we observe that at semi peripheral collisions multiplicity <IMF> shows a peak because most of the spectator source does not take part in collision and large number of IMF's are observed. For central geometry the collisions are violent so there few number of IMF's observed and for peripheral collisions very small portion of target and projectile overlap so again few number of IMF's observed most of the fragments goes out in heavy mass fragments (HMF's). In this way we get a clear '*rise and fall'* in multifragmentation emission. The variation of the IMF's match with the experimental data when the distance between the nucleon is 4 fm. Because the peak point of the variation of IMF's at this distance is approximately match with experimental peak. It is observed that IMF's shows the agreement with data at low impact parameters but fails at intermediate impact parameters. This failure is due to the drawbacks in the method of analysis MST which we had used in our analysis. MST method gives the heavy cluster at the time of high densities.

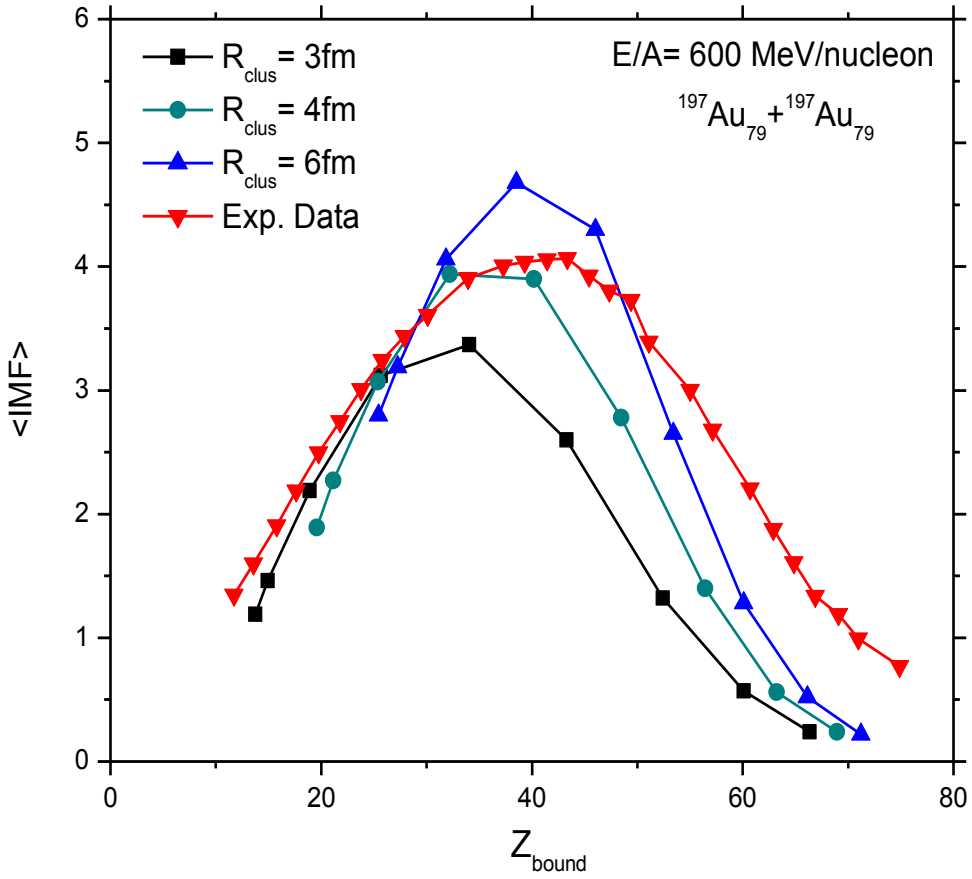

Fig.3.14.Multiplicity of IMF's as a function of Z_{bound} .

Chapter 4

Summary and outlook

In **chapter 1.** This thesis contains a theoretical study of multifragmentation of the five reactions $^{20}Ne_{10}$ +$^{20}Ne_{10}$, $^{40}Ca_{20}$ + $^{40}Ca_{20}$, $^{91}Zr_{40}$ +$^{91}Zr_{40}$, $^{131}Xe_{54}$ + $^{131}Xe_{54}$ and $^{197}Au_{79}$ + $^{197}Au_{79}$. Isospin Quantum Molecular Dynamics (IQMD) is used to study these reactions at 100 MeV/nucleon and 600 MeV/nucleon energy and at different scaled impact parameters (0.0, 0.3, 0.6, 0.9). A brief introduction of multifragmentation is also discussed.

In **chapter 2.** We have discussed the IQMD model and momentum dependent interaction for our present study.

In **chapter 3**. We have studied the detailed analysis of multifragmentation. Different parameters like time evolution, impact parameter dependence, energy dependence with variation of R_{clus} is studied for free nucleon & LMF's and IMF's. It is concluded that free nucleon & LMF's have a different trend as compare to IMF's. This is due to different origin of their formation. The rise and fall in the multiplicity of IMF's is observed. The rise & fall is further compared with the experimental data of ALADIN and are found to be in close agreement at low impact parameter. Disagreement at higher impact parameter is due to unavailability of experimental filters. Spatial correlations plays significant role in deciding the fragment configuration. It has been observed that maximum production of LMF's take place at R_{clus}= 4 fm. Our investigations shows that further studies with along with momentum constraints can be a better tool to pin down the multifragmentation.

References

[1]. C. Hartnack, Rajiv K Puri, J. Aichelin, J Konopka, S. A. Bass, H. Stocker, W. Greiner, Eur Phys. J. A **1**, 151(1998); R K Puri *et al*, *Nucl. Phys.* **A 575**, 733 (1994); V. kaur, S. Kumar & R. K. Puri, PL **B 697**, 512(2011).

[2]. L. C. Vaz, J. M. Alexander and G. R. Satchler, Phys. Rep. **69,** 373(1981); M. Beckerman, Rep. Prog. Phys. **51**, 1047 (1988).

[3]. K. E. Zyromski et al., Phys. Rev. **C 55**, R562 (1997).

[4]. C. Ngo, B. Tamain, M. Breiner, R. J. Lombard, D. Mas, and H. H. Deubler, Nucl. Phys**. A 252**, 237 (1975); H. Ngo and C.h. Ngo, Nucl. Phys. **A 348**, 140(1980); K. C. Panda and T. Patra, J. Phys. **G 14**, 1489 (1988).

[5]. See e.g. Heavy Elements and Related New Phenomena Vol. 1 and Vol.2 eds, W. Greiner and R. K. Gupta, World Scientific, Singapore(1999).

[6]. R. K. Gupta, S. Singh, R. K. Puri and W. Scheid, *Phys. Rev.* **C 47**, 561 (1993); R. K. Gupta *et al*, *J. Phys. G: Nucl. Part.* **18**, 1533 (1992); S. S. Malik, S. Singh, R. K. Puri, S. Kumar and R. K. Gupta, *Pramana - J. Phys.* **32**, 419 (1989); R. K. Puri, S. S. Malik and R. K. Gupta, *Eur. Phys. Lett.* **9**, 767 (1989); R. K. Puri and R. K. Gupta, *Phys. Rev.* **C45**, 1837(1992); R. K. Puri *et al*, *Eur. Phys. J.* **A23**, 429(2005).

[7]. H. Stoker and W. Greiner, Phys. Rep. **137**, 277(1986).

[8]. J. P. Bonder, A. S. Bovina, A. S. Illinova, I. N. Misusing, and K. Snapped, Phys. Rep. **257**, 133 (1995). S. Pal, S. K. Samaddar, and J. N. De, Nucl. Phys. **A 608**, 49(1996), D. K. Srivastava et al., [Nucl-th] 0506075(2005); L. Satpathy, M. Mishra, A. Das, M. Satpathy, Phys.Lett. **B 237**, 181 (1990); C. B. Das, A. Das, L. Satpathy, M. Satpathy, Phys. Rev. **C 53**, 1833 (1996)

[9]. D. H. E. Gross, Rep. Prog. Phys. **53**, 605 (1990).

[10]. G. F. Bertsch, H. Kruse and S. D. Gupta, Phys. Rev. C **29**, R673 (1984); J. J. Molitoris, H. Stocker, and B. L. Winer, Phys. Rev. C **36**, 220 (1987); C. Gale et. al, Phys. Rev.**C**

41, 1545 (1990); W. Cassing, W. Metag, U. Mosel, and K. Nitta, Phys. Rep. **188**, 363 (1990).

[11]. E. Suraud, C. Gregoire, and B. Tamain, Prog. Part. Nucl. Phys. **23**, 357 (1989).

[12]. G. Batico, J. Radrup and T. Vetter, Nucl. Phys. **A 536**, 786 (1992).

[13]. L. Wilets, Y. Yariv, and R. Chestnut, Nucl. Phys. **A 301**, 359 (1978); A. R. Bodmer, C. N. Panos, and A. D. MacKellar, Phys. Rev. **C 22**, 1025 (1980); A. Vicentini, G. Jacucci and V. R. Pandharipande, Phys. Rev. **C 31**, 1783(1985).

[14]. J. Aichelin et al., Phys. Rev. Lett. **58**, 1926 (1987); J. Aichelin et al., Phys. Rev. **C 37**, 2451 (1988); L. Zhuxia, C.Hartnack, H. Stocker and W. Greiner, Phys. Rev. **C 44**, 824 (1991); D. T. Khoaetal., Nucl. Phys. **A 529**, 363(1991); G. Q. Li *et al*., Nucl. Phys. **A 534**, 697 (1991); G. Q. Li *et al*., Nucl. Phys. **A 537**, 631 (1992); S. Huber and J. Aichelin, Nucl. Phys. **A 573**, 587(1994); C. Fuchs, A. Faessler, E. Zabrodin, and Y. M. Zheng, Phys. Rev. Lett. **86**, 1974(2001); E. Lehmann *et al*., Phys. Rev. **C 51**, 2113 (1995); E. Lehmann *et al*., Z Phys. **A 355**, 55(1996).

[15]. J. Aichelin Phys. Rep. **202**, 233 (1991); R K Puri, C. Hartnack and J. Aichelin, *Phys. Rev.* **C54**, R28 (1996); P B Gassiaux *et al*, *Nucl. Phys.* **A619**, 379 (1997); R K Puri and J. Aichelin, *J. Comp. Phys.* **162**, 245(2000); Y K Vermani, S Goyal and R K Puri, *J. Phys. G: Nucl. Part.* **36**, 105103 (2009); Y K Vermani and R K Puri, *Eur. Phys. Lett.* **85**, 62001(2009).

[16]. B. A. Li *et al*., Phys. Rev. **C 52**, R1746 (1995).

[17]. M. Colonna *et al*., Phys. Rev. **C 57**, 1410 (1998).

[18]. E. Schopper, Naturwissenschaftler **5**, 557 (1937); I. I. Gurevich et al., Dokl. Akad. Nauk SSSR **18**, 169(1938).

[19]. B. Jakobsson *et al*., Z. Phys. **A 307**, 293 (1982).

[20]. A. I. Warwick *et a*l., Phys. Rev. **C 27**, 1083 (1983).

[21]. J. E. Finn *et al*., Phys. Rev. Lett. **49**, 1321 (1982).

[22]. J. P. Alard *et al*., Phys. Rev. Lett. **69**, 889 (1992).

[23]. E. Lehmann, R. K. Puri, A. Feassler, G. Batko and W. Huang, Phys. Rev. **C 51**, 2113(1995).

[24]. A. Bohnet, N. Ohtsuka, J. Aichelin, R. Linden A. Feassler, Nucl. Phys. **A 494**, 349 (1989); J. Jaenicke, J. Aichelin, N. Ohtsuka, R. Linden and A. Feassler, Nucl. Phys. **A 536**, 201 (1992).

[25]. L. Wilets, Y. Yariv and R. Chest nut; Nucl. Phys. **A301**, 359(1978).

[26]. R. K. Puri, C. Hartnack, and J. Aichelin, Phys. Rev. **C 54**, R28 (1996); P. B. Gossiaux, R. Puri, C. Hartnack, and J. Aichelin, Nucl. Phys. **A 619**, 379(1997).

[27]. C. Dorso and J. Randrup, Phys. Lett. **B 301**, 328(1993).

[28]. Sanjeev Kumar, Suneel Kumar, and Rajeev K. Puri, Physical Review **C 78**, 064602 (2008).

[29]. C. Hartnack, H. Oeschler, and J. Aichelin, Phys. Rev. Lett. **90**, 102302 (2003); J. Phys G: Nucl. and Part. Phys. **35**, 044021 (2008).

[30]. J. Singh, S. Kumar and R. K. Puri, *Phys. Rev.* **C62**, 044617 (2000); S Kumar and R K Puri, *ibid.* **58**, 1618 (1998); Y K Vermani, S Goyal and R K Puri, *ibid.* **79**, 064613 (2009).

[31]. S. Kumar and R. K. Puri, Phys. Rev. C **60**, 054607 (1999); Y. K.Vermani and Rajeev K. Puri, Phys. Rev. **C 78**, 064602(2008).

[32]. J. Singh, S. Kumar, and R. K. Puri, Phys. Rev**. C 63**, 054603 (2001).

[33]. S. Kumar and R. K. Puri, Phys. Rev. **C 58,** 320 (1998); DAE Symposium on Nuclear Phys. **40** B, p.152 (1997).

[34]. S. R. Souza, L. de Paula, S. Leray, J. Nemeth, C. Ngo, and H. Ngo, Nucl. Phys. **A 571**, 159(1994).

[35]. C. Sfienti et. al. Acta Physica polonica **B 37** (2006).

[36]. C. A. Ogilvie et al., Phys. Rev. Lett. **67**, 1214 (1991).